

25. Hao H-X, Xie Y, Zhang Y, Charlat O, Oster E, et al. (2012) ZNRF3 promotes Wnt receptor turnover in an R-spondin-sensitive manner. *Nature* 485: 195–200.
26. Koo B-K, Spit M, Jordens I, Low TY, Stange DE, et al. (2012) Tumour suppressor RNF43 is a stem-cell E3 ligase that induces endocytosis of Wnt receptors. *Nature* 488: 665–669.
27. Wu J, Jiao Y, Dal Molin M, Maitra A, de Wilde RF, et al. (2011) Whole-exome sequencing of neoplastic cysts of the pancreas reveals recurrent mutations in components of ubiquitin-dependent pathways. *Proc Natl Acad Sci U S A* 108: 21188–21193.
28. Furukawa T, Kuboki Y, Tanji E, Yoshida S, Hatori T, et al. (2011) Whole-exome sequencing uncovers frequent GNAS mutations in intraductal papillary mucinous neoplasms of the pancreas. *Sci Rep* 1: 161. Available: <http://www.nature.com/srep/2011/111118/srep00161/full/srep00161.html>. Accessed 5 April 2012.
29. Ong CK, Subimerb C, Pairojkul C, Wongkham S, Cutcutache I, et al. (2012) Exome sequencing of liver fluke-associated cholangiocarcinoma. *Nat Genet* 44: 690–693.
30. Muzny DM, Bainbridge MN, Chang K, Dinh HH, Drummond JA, et al. (2012) Comprehensive molecular characterization of human colon and rectal cancer. *Nature* 487: 330–337.
31. Ryland GL, Hunter SM, Doyle MA, Rowley SM, Christie M, et al. (2012) RNF43 is a tumour suppressor gene mutated in mucinous tumours of the ovary. *J Pathol* 229: 469–476.
32. Yagy R, Furukawa Y, Lin YM, Shimokawa T, Yamamura T, et al. (2004) A novel oncoprotein RNF43 functions in an autocrine manner in colorectal cancer. *Int J Oncol* 25: 1343–1348.
33. Lin YM, Furukawa Y, Tsunoda T, Yue CT, Yang KC, et al. (2002) Molecular diagnosis of colorectal tumors by expression profiles of 50 genes expressed differentially in adenomas and carcinomas. *Oncogene* 21: 4120–4128.
34. van der Flier LG, Sabates-Bellver J, Oving I, Haegbarth A, De Palo M, et al. (2007) The Intestinal Wnt/TCF Signature. *Gastroenterology* 132: 628–632.
35. van de Wetering M, Sancho E, Verweij C, de Lau W, Oving I, et al. (2002) The β -Catenin/TCF-4 Complex Imposes a Crypt Progenitor Phenotype on Colorectal Cancer Cells. *Cell* 111: 241–250.
36. Hatzis P, van der Flier LG, van Driel MA, Guryev V, Nielsen F, et al. (2008) Genome-wide pattern of TCF7L2/TCF4 chromatin occupancy in colorectal cancer cells. *Mol Cell Biol* 28: 2732–2744.
37. Yochum GS (2011) Multiple Wnt/beta-Catenin Responsive Enhancers Align with the MYC Promoter through Long-Range Chromatin Loops. *PLoS One* 6: e18966.
38. Yochum GS, McWeeney S, Rajaraman V, Cleland R, Peters S, et al. (2007) Serial analysis of chromatin occupancy identifies beta-catenin target genes in colorectal carcinoma cells. *Proc Natl Acad Sci U S A* 104: 3324–3329.
39. Bottomly D, Kyler SL, McWeeney SK, Yochum GS (2010) Identification of beta-catenin binding regions in colon cancer cells using ChIP-Seq. *Nucleic Acids Res* 38: 5735–5745.
40. Jho EH, Zhang T, Domon C, Joo CK, Freund JN, et al. (2002) Wnt/beta-catenin/Tcf signaling induces the transcription of Axin2, a negative regulator of the signaling pathway. *Mol Cell Biol* 22: 1172–1183.
41. Leung JY, Kolligs FT, Wu R, Zhai Y, Kuick R, et al. (2002) Activation of AXIN2 expression by beta-catenin-T cell factor. A feedback repressor pathway regulating Wnt signaling. *J Biol Chem* 277: 21657–21665.
42. Lustig B, Jerchow B, Sachs M, Weiler S, Pietsch T, et al. (2002) Negative feedback loop of Wnt signaling through upregulation of conductin/axin2 in colorectal and liver tumors. *Mol Cell Biol* 22: 1184–1193.
43. Niida A, Hiroko T, Kasai M, Furukawa Y, Nakamura Y, et al. (2004) DKK1, a negative regulator of Wnt signaling, is a target of the beta-catenin/TCF pathway. *Oncogene* 23: 8520–8526.
44. González-Sancho JM, Aguilera O, García JM, Pendás-Franco N, Peña C, et al. (2005) The Wnt antagonist DICKKOPF-1 gene is a downstream target of beta-catenin/TCF and is downregulated in human colon cancer. *Oncogene* 24: 1098–1103.
45. Suzuki H, Watkins DN, Jair KW, Schuebel KE, Markowitz SD, et al. (2004) Epigenetic inactivation of SFRP genes allows constitutive WNT signaling in colorectal cancer. *Nat Genet* 36: 417–422.

Overexpression of Cohesion Establishment Factor DSCC1 through E2F in Colorectal Cancer

Kiyoshi Yamaguchi^{1*}, Rui Yamaguchi², Norihiko Takahashi¹, Tsuneo Ikenoue¹, Tomoaki Fujii¹, Masaru Shinozaki³, Giichiro Tsurita³, Keisuke Hata³, Atsushi Niida⁴, Seiya Imoto⁴, Satoru Miyano^{2,4}, Yusuke Nakamura⁵, Yoichi Furukawa¹

1 Division of Clinical Genome Research, Advanced Clinical Research Center, Institute of Medical Science, The University of Tokyo, Tokyo, Japan, **2** Laboratory of Sequence Analysis, Human Genome Center, Institute of Medical Science, The University of Tokyo, Tokyo, Japan, **3** Department of Surgery, Research Hospital, Institute of Medical Science, The University of Tokyo, Tokyo, Japan, **4** Laboratory of DNA Information Analysis, Human Genome Center, Institute of Medical Science, The University of Tokyo, Tokyo, Japan, **5** Laboratory of Molecular Medicine, Human Genome Center, Institute of Medical Science, The University of Tokyo, Tokyo, Japan

Abstract

Ctf18-replication factor C complex including Dscc1 (DNA replication and sister chromatid cohesion 1) is implicated in sister chromatid cohesion, DNA replication, and genome stability in *S. cerevisiae* and *C. elegans*. We previously performed gene expression profiling in primary colorectal cancer cells in order to identify novel molecular targets for the treatment of colorectal cancer. A feature of the cancer-associated transcriptional signature revealed from this effort is the elevated expression of the proto-oncogene *DSCC1*. Here, we have interrogated the molecular basis for deviant expression of human *DSCC1* in colorectal cancer and its ability to promote survival of cancer cells. Quantitative PCR and immunohistochemical analyses corroborated that the expression level of *DSCC1* is elevated in 60–70% of colorectal tumors compared to their matched noncancerous colonic mucosa. An *in silico* evaluation of the presumptive *DSCC1* promoter region for consensus DNA transcriptional regulatory elements revealed a potential role for the E2F family of DNA-binding proteins in controlling *DSCC1* expression. RNAi-mediated reduction of E2F1 reduced expression of *DSCC1* in colorectal cancer cells. Gain- and loss-of-function experiments demonstrated that *DSCC1* is involved in the viability of cancer cells in response to genotoxic stimuli. We reveal that E2F-dependent expression of *DSCC1* confers anti-apoptotic properties in colorectal cancer cells, and that its suppression may be a useful option for the treatment of colorectal cancer.

Citation: Yamaguchi K, Yamaguchi R, Takahashi N, Ikenoue T, Fujii T, et al. (2014) Overexpression of Cohesion Establishment Factor DSCC1 through E2F in Colorectal Cancer. PLoS ONE 9(1): e85750. doi:10.1371/journal.pone.0085750

Editor: Srikumar P. Chellappan, H. Lee Moffitt Cancer Center & Research Institute, United States of America

Received: October 28, 2013; **Accepted:** November 30, 2013; **Published:** January 17, 2014

Copyright: © 2014 Yamaguchi et al. This is an open-access article distributed under the terms of the Creative Commons Attribution License, which permits unrestricted use, distribution, and reproduction in any medium, provided the original author and source are credited.

Funding: This work was supported in part by Grant-in-Aid for Young Scientists (#23790126), MEXT/JSPS, Japan to K. Yamaguchi, and Global COE Program “Center of education and research for the advanced genome-based medicine for personalized medicine and the control of worldwide infectious diseases”, MEXT/Japan Society for the Promotion of Science, Japan to Y. Furukawa. The funders had no role in study design, data collection and analysis, decision to publish, or preparation of the manuscript.

Competing Interests: The authors have declared that no competing interests exist.

* E-mail: kiyamagu@ims.u-tokyo.ac.jp

Introduction

Colorectal cancer (CRC) is one of the most frequent human neoplasms in the world. In CRC cells, disruption of systems governing genetic or epigenetic integrity renders different features such as chromosomal instability (CIN), microsatellite instability (MSI), and CpG island methylator phenotype (CIMP). A great majority of colorectal tumors exhibit CIN that includes gross genetic changes such as deletions, amplifications, inversions, rearrangements, gain or loss of whole or large portions of chromosomes, and translocations [1]. An earlier study identified somatic mutations in five genes including *MRE11*, *ZW10*, *ZWILCH*, *ROD*, and *DING*, among 100 human CIN-candidate genes that shared similarity with yeast or fly “instability” genes [2]. Their data suggested that at least one of three functions including double-strand break repair, kinetochore function, and chromatid segregation, is impaired in CIN tumors by somatic mutation. Another study searched for mutations of 102 human homologues of yeast CIN genes in 132 colorectal cancers. Consequently, they identified a total of 11 mutations in five genes that included four associated with sister chromatid cohesion (*SMC1L1*, *CSPG6*,

NIPBL, and *STAG3*, the homologues of yeast *SMC1*, *SMC3*, *SCC2*, and *SCC3*, respectively) [3]. Since sister chromatid cohesion is indispensable for cellular processes such as chromosome segregation, homologous recombinational repair, and regulation of transcription [4], genetic alterations in the components and regulators should play a crucial role in the CIN of colorectal tumors.

We previously performed gene expression profile analysis in CRC [5], and identified that DNA replication and sister chromatid cohesion 1 (*DSCC1*, also known as *DCCI*) was frequently elevated in colorectal tumors compared with non-cancerous colonic mucosa. Dcc1p, a homolog of *DSCC1*, was first identified as a member of alterative replication factor C (RFC) complex in the yeast, and physically associates with Ctf8p and Ctf18p [4]. Deletion of the component, Ctf18p, Ctf8p, or Dcc1p, resulted in severe sister chromatid cohesion defects, and increased sensitivity to microtubule depolymerizing drugs, suggesting that these components are essential for maintenance of chromatin integrity [4]. Although Dcc1p was not essential for the viability of yeast, deletion of Dcc1p led to synthetic lethality in combination

with mutation of other sister chromatid cohesion proteins [6]. In addition to the implication in sister chromatid cohesion, the CTF18-DSCC1-CTF8-RFC complex plays a crucial role in DNA replication through the interaction with single-stranded and primed DNA as a loader of proliferating cell nuclear antigen [7]. Furthermore, genetic network analysis of functionally related genes in the yeast suggested that the components of CTF18-DSCC1-CTF8-RFC complex interact with the MAD/BUB spindle checkpoint pathway, the RAD51 DNA repair pathway for double-strand breaks, the RAD9 DNA damage checkpoint, and the TOF1/MRC DNA replication checkpoint pathway [8,9]. The finding that mutation in CTF18-RFC increased triplet repeat instability corroborated the role of this complex in the DNA-replication checkpoint [10]. These data indicated that DSCC1 plays an important role in replication, spindle checkpoint and DNA repair, which prompted us to investigate whether deregulated expression of DSCC1 is involved in human colorectal tumorigenesis.

Here, we show for the first time that DSCC1 is frequently up-regulated in CRC at least in part through the enhanced transcriptional activation by E2F. We also reveal that elevated expression of DSCC1 confers chemoresistance in CRC cells by providing tumor cells with anti-apoptotic properties. These findings will contribute to a better understanding of CRC, and serve as a starting point for the development of novel strategies for diagnosis and treatment of CRC.

Materials and Methods

Ethics statement

This project was approved by the ethical committee of Institute of Medical Science, the University of Tokyo (IMSUT-IRB, 21-14-0806). Written informed consent was obtained from all patients in this study. All colorectal cancer tissues and corresponding non-cancerous tissues were obtained from surgical specimens of patients who underwent surgery.

Cell culture

Human CRC cell lines HCT116, HCT-15, SW480, DLD-1, LoVo, Caco-2, LS174T, HT-29, and RKO were purchased from the American Type Culture Collection (Manassas, VA). All cells were grown in appropriate media supplemented with FBS (Life Technologies, Carlsbad, CA) and antibiotic/antimycotic solution (Sigma, St. Louis, MO).

Preparation of plasmids expressing DSCC1 and E2Fs

The entire coding region of *DSCC1* cDNA (GenBank accession No. NM_024094) was amplified by RT-PCR using a set of primers; forward primer: 5'-CCGGAATTCATGAAGAG-GACCCGCGAC-3' and reverse primer: 5'-CGGCTCGAGA-GAAATGGGTCTTCTCGAATTAT-3' (underlined nucleotides indicate the recognition sites of restriction enzymes). The PCR products were cloned into the *EcoRI* and *XhoI* sites of pcDNA3.1/myc-His. We additionally generated plasmids expressing HA-tagged DSCC1 (pCAGGS-DSCC1). The constructs pcDNA3-HA-E2Fs were kindly provided by Dr. J. R. Nevins (Duke University, Durham, NC).

Quantitative PCR and gene copy number analysis

Real-time PCR was performed using the LightCycler 480 system (Roche Diagnostics, Indianapolis, IN). Genomic DNAs were extracted from CRC cell lines for copy number analysis. Quantitative PCR was performed on ABI PRISM 7900HT Sequence Detection System, using FAM-labeled probes (5'-

TCAGGTTTCTCTACCTTCCGGCTGCTT-3') and a set of primers (forward: 5'-GGCGCGCTTCAAACG-3', reverse: 5'-GCGGGCAAGAAAGAAGTTCC-3') for *DSCC1*, and TaqMan Copy Number Reference Assays RNase P as a quantitative control (Life Technologies). The copy number of *DSCC1* in the cancer cells was calculated in comparison with genomic DNA from healthy volunteers using CopyCaller Software.

Subcellular fractionation and immunoblotting

Cells were lysed in radioimmunoprecipitation assay buffer (50 mM Tris-HCl, pH 8.0, 150 mM NaCl, 0.5% sodium deoxycholate, 1% Nonidet P-40, 0.1% SDS) supplemented with a Protease Inhibitor Cocktail Set III (Calbiochem, San Diego, CA). Nuclear extracts were prepared using Nuclear Extract Kit (Active Motif, Carlsbad, CA). Proteins were separated by SDS-PAGE and immunoblot analysis was performed using the indicated antibodies. Horseradish peroxidase-conjugated goat anti-mouse or anti-rabbit IgG (GE Healthcare, Buckinghamshire, UK) served as the secondary antibody for the ECL Detection System (GE Healthcare).

Immunostaining

Primary antibodies used for immunohistochemical and immunocytochemical staining were anti-DSCC1 (B01P, Abnova, Taipei, Taiwan) and anti-Myc (Sigma). The specificity of DSCC1 antibody was confirmed by the blocking with DSCC1 recombinant protein (data not shown). These experiments were performed as described previously [11].

Induction of apoptosis and flow cytometry

To study the induction of apoptosis, cells were treated with camptothecin (Wako, Osaka, Japan), doxorubicin (LC Laboratories, Woburn, MA), MG132 (Merck Millipore, Darmstadt, Germany), or exposed to γ -irradiation (Gammacell 40, Atomic Energy of Canada, Ontario, Canada). Expression of cleaved poly (ADP-ribose) polymerase (PARP) and cleaved caspase-3 was detected by western blot analysis using anti-cleaved PARP (9541) and anti-caspase-3 antibodies (9662), respectively (Cell Signaling Technology, Danvers, MA). Assessment of apoptosis was also performed by annexin V and PI double-staining using Alexa Fluor 488 Annexin V/Dead Cell Apoptosis Kit (Life Technologies). Briefly, cultured cells were treated with vehicle or camptothecin for 24 h. The cells were stained with Annexin V and PI, and subsequently analyzed on a FACSCalibur (Becton Dickinson, Franklin Lakes, NJ) using FlowJo software (Tree Star, Ashland, OR).

Cell viability assay

Plasmids expressing short hairpin RNA (shRNA) using U6 promoter (*psiU6BX3.0*) were prepared as described previously [12]. Plasmids expressing DSCC1 shRNA (*psiU6-shDSCC1*) were constructed by cloning double-stranded oligonucleotides into the *BbsI* sites of the *psiU6BX3.0* vector. Two target sequences, 5'-GUGGACAGAAGAAGAUUU-3' (*shDSCC1#1*) and 5'-GCAAACCAUAGGUGCAUUA-3' (*shDSCC1#2*), were used for DSCC1 shRNAs. As negative controls, we prepared a plasmid targeting enhanced green fluorescent protein (*psiU6-shEGFP*) and those targeting scrambled sequences of *shDSCC1#1* (5'-AAAUUGCGAAGGUGAUGAA-3'; *psiU6-shDSCC1#1scr*) or *shDSCC1#2* (5'-AACACGUUAAUACCGGUG-3'; *psiU6-shDSCC1#2scr*). Cell viability assays were carried out as described previously using HCT116, SW480, and RKO cells transfected with plasmids expressing shEGFP, shDSCC1, or

scramble shDSCC1 [11]. To investigate the effect of DSCC1 overexpression on cell proliferation, we transfected SW480 and HCT116 cells with pCAGGS-DSCC1 and established two or three clones stably expressing exogenous DSCC1. Control SW480 and HCT116 cells transfected with empty vector were also established as mock cells.

Promoter reporter assays and site-directed mutagenesis

Luciferase reporter plasmids containing the *DSCC1* promoter were prepared by cloning the 5'-flanking region of *DSCC1* into the *MluI* and *BglII* restriction enzyme sites of pGL3-Basic vector (Promega, Madison, WI). A DNA fragment of approximately 1.0-kb in the 5'-flanking region of *DSCC1* was amplified by PCR using genomic DNA from healthy volunteers and a set of primers (forward: 5'-CGACGCGTATGTCTGCTCAGATCCTTTGAAT-3', reverse: 5'-GAAGATCTCGCCGGGTCTAGAGTCC-3'). Mutant plasmids containing substitutions in putative E2F binding sites of the *DSCC1* promoter were generated by site-directed mutagenesis using the QuikChange II XL Site-Directed Mutagenesis Kit (Agilent Technologies, Santa Clara, CA). Cells seeded into 6-well plates were transfected with the reporter plasmids together with pRL-TK (Promega) using FuGENE 6 reagent. Cells were harvested 24 hours after transfection, and reporter activities were measured by dual luciferase system (TOYO B-Net, Tokyo, Japan). For the knock-down of E2F1 expression, synthetic E2F1 siRNA was purchased from Sigma (sense: 5'-GGGAGAAGUCACGCUAUGA-3', antisense: 5'-AUAGCGUGACUUCUCCCCC-3').

Chromatin immunoprecipitation assay

To investigate the interaction of E2F1 with the *DSCC1* promoter region, a chromatin immunoprecipitation (ChIP) assay was performed according to the Agilent Mammalian ChIP protocol with slight modifications. HCT116 cells were cross-linked with 1% formaldehyde for 10 min at room temperature and quenched with 0.4 M glycine. Chromatin extracts were sheared by micrococcal nuclease digestion, and subsequently protein-DNA complexes were immunoprecipitated with 3 µg of anti-E2F1 polyclonal antibody (C-20, Santa Cruz Biotechnology, Santa Cruz, CA) bound to anti-rabbit IgG-coated Dynabeads (Life Technologies). Non-immune rabbit IgG (Santa Cruz Biotechnology) was used as a negative control. The precipitated DNAs were subjected to quantitative PCR analysis with a primer set (forward (-26) 5'-CCGGAACACGCCCCATGGC-3' and reverse (+127) 5'-GGGTCTCTTCATCGCAGC-3') to amplify the *DSCC1* promoter region. Specificity of the assay was determined by the amplification of a distal upstream region in the *DSCC1* promoter with the following primers: forward (-1279) 5'-AGTTGTAGGGAATGTTTCCCATT-3' and reverse (-1111) 5'-GATTGGTTTCATGTGACCTACTTC-3'. In addition, the amplifications of cell division cycle 2 (*CDC2*) promoter and glyceraldehyde-3-phosphate dehydrogenase (*GAPDH*) promoter were used for positive and negative controls, respectively (primers: *CDC2* forward 5'-CGCCCTTTCCTCTTTCTTTC-3', *CDC2* reverse 5'-ATCGGGTAGCCCGTAGACTT-3', *GAPDH* forward 5'-TACTAGCGGTTTTACGGGCG-3', *GAPDH* reverse 5'-TCGAACAGGAGGAGCAGAGCGGA-3').

Results

Expression of DSCC1 is frequently elevated in CRC

In order to identify novel target molecules for the treatment and/or diagnostic biomarkers of CRC, we previously performed expression profile analysis of colorectal tumors and their matched

normal colorectal tissues by cDNA microarray [5]. Among the genes deregulated in colorectal tumors, expression of DNA replication and sister chromatid cohesion 1 (*DSCC1*) was increased more than two-fold in 5 of 7 colorectal cancers compared with corresponding non-cancerous colon mucosa (Figure 1A). Subsequent real-time PCR analysis using an additional 20 CRC tissues and the corresponding non-cancerous mucosa revealed that *DSCC1* expression was elevated more than two-fold in 12 of the 20 tumors (Figure 1A). An immunohistochemical staining showed accumulated DSCC1 protein in 29 of 40 CRC tissues compared with corresponding adjacent non-cancerous colonic mucosa (Figure 1B). Although we searched for correlations between its expression and clinicopathological factors including age and sex of the patients, location, size, and histological data of the tumors such as depth of invasion, lymph node involvement, and vascular or lymphatic vessel invasion, none of the factors was significantly associated with DSCC1 expression (Table S1). Additionally, western blot analysis using CRC cell lines revealed that DSCC1 was abundantly expressed in HCT116, HT-29, and DLD-1 cells, and that it was expressed at low levels in SW480, SW620, and Caco-2 cells (Figure 1C). Although we compared stability of DSCC1 protein in HCT116 (DSCC1-high) and SW480 (DSCC1-low) cells by cycloheximide chase assay, DSCC1 was relatively stable in both HCT116 and SW480 cells. Treatment with MG132, a proteasome inhibitor also did not enhance DSCC1 expression (Figure S1A). These data suggested that protein stability is not likely to play a major role in the elevated expression of DSCC1 in cancer cells.

Immunohistochemical analysis unexpectedly depicted accumulated DSCC1 in the cytoplasm and nucleus of DSCC1-positive cancer cells (Figure 1B), although Dsccl1 was reported to play a role in the establishment of cohesion during DNA replication in the yeast. To elucidate its subcellular localization, we carried out immunocytochemical staining of endogenous DSCC1 in HCT116 cells. Consistent with the immunohistochemical staining of cancer tissues, DSCC1 protein was localized in both cytoplasm and nucleus (Figure 1D and S1B). Furthermore, western blot analysis using cytoplasmic and nuclear fractions extracted from HCT116, RKO, and DLD-1 cells (Figure 1E) and cells expressing Myc-tagged DSCC1 confirmed its subcellular localization in the cytoplasm as well as the nucleus (Figure S1C and S1D).

Copy number analysis of DSCC1

To address whether gene amplification is involved in the DSCC1 overexpression, we conducted copy number analysis by quantitative PCR using RNase P as a control. Compared with peripheral leukocytes from healthy volunteers, the copy number of *DSCC1* was not increased in any CRC cell lines tested (Figure 1F). It is worth noting that a decrease in copy number was observed in HT-29 cells that abundantly expressed DSCC1 (Figure 1C). We further analyzed copy number alteration of *DSCC1* in colon and rectum adenocarcinoma (The Cancer Genome Atlas Colorectal Cancer project) using the cBioPortal database (<http://www.cbioportal.org/public-portal/>). As a result, putative copy number changes were found in 7 of 257 colorectal adenocarcinomas (2.7%), suggesting that amplification of *DSCC1* does not play a major role in the enhanced DSCC1 expression.

Regulation of DSCC1 promoter activity

To resolve the mechanism of elevated DSCC1 expression in CRC, we investigated the promoter activity of *DSCC1* in HCT116 cells. Reporter assay using plasmids containing a 5'-flanking region of *DSCC1* (pDSCC1-1023/+109) showed that this region has a substantial promoter activity (data not shown). In the region,

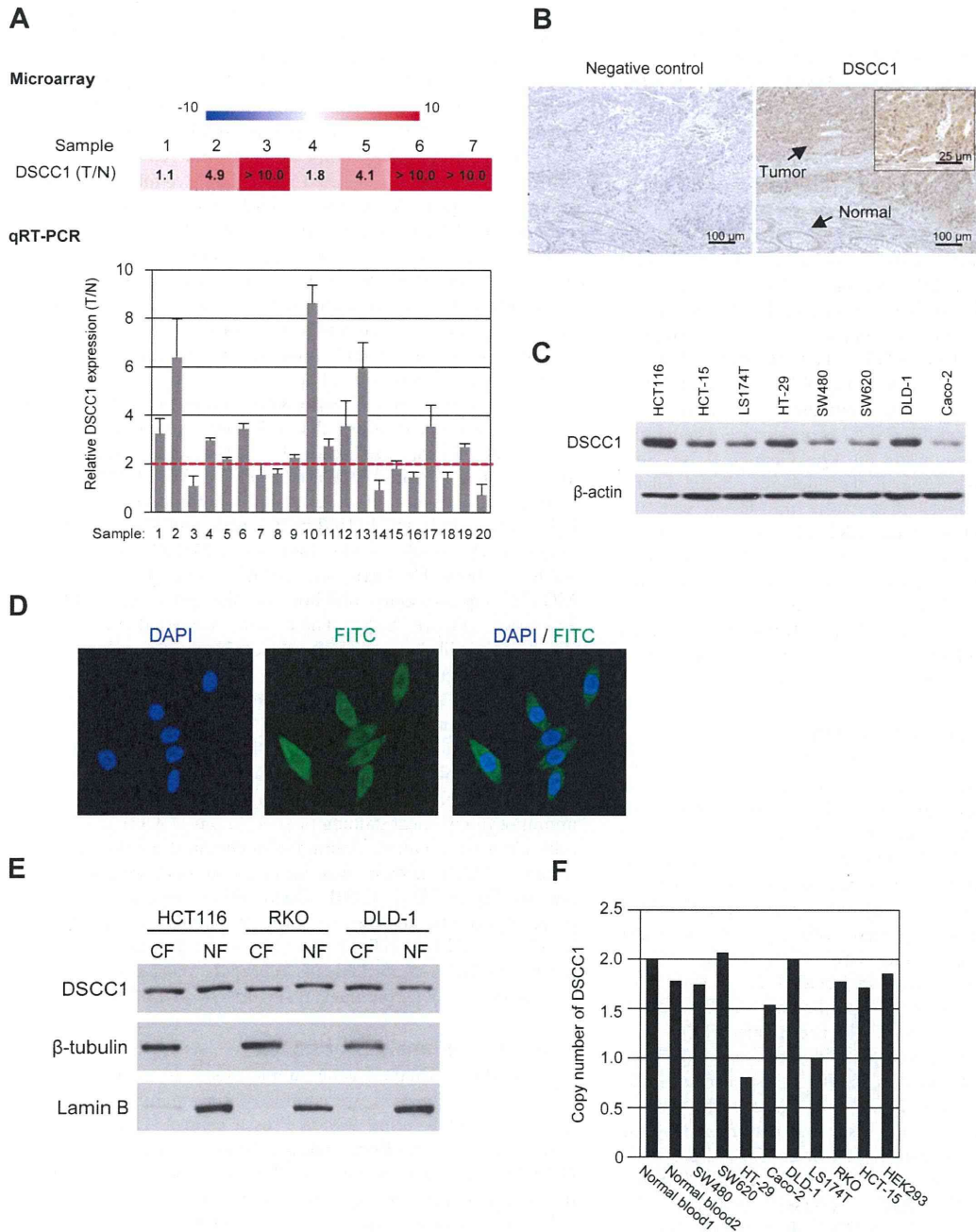


Figure 1. Expression of DSCC1 in colorectal tumors. (A) Relative expression ratios of *DSCC1* in seven colorectal cancer tissues to their corresponding normal tissues in our microarray data (upper panel). Relative expression levels of *DSCC1* in an additional 20 colorectal tumors and the corresponding non-cancerous mucosa was analyzed by quantitative PCR (lower panel). Quantity of *DSCC1* was normalized to *HPRT1* expression. Y axis indicates the ratio of mean of *DSCC1* expression in tumor to that in their corresponding normal tissue. The data represents mean \pm SD from triplicate experiments. (B) Representative image of immunohistochemical staining of *DSCC1* in a human colon cancer tissue containing cancer cells and adjacent normal mucosa. (C) Expression of *DSCC1* in CRC cell lines was detected by western blotting using anti-*DSCC1* antibody. (D) HCT116 cells were probed with anti-*DSCC1* antibody followed by FITC-conjugated anti-mouse IgG secondary antibody (green). Nuclei were counter-stained with DAPI (blue). (E) HCT116, RKO, and DLD-1 cells were separated into the cytoplasmic (CF) and nuclear fractions (NF), and the cytoplasmic and nuclear proteins were subjected to SDS-PAGE followed by western blotting. Purity of the fractions was determined by the presence of β -tubulin (cytoplasmic marker) and lamin B (nuclear marker). (F) Copy number analysis of *DSCC1* in eight CRC cell lines and HEK293 cells. Relative copy number of *DSCC1* gene was determined by quantitative PCR using *RPPH1* as an endogenous reference. The copy number was calculated by dividing their PCR products by those of peripheral leukocytes from healthy volunteers, and subsequently multiplying by 2.
doi:10.1371/journal.pone.0085750.g001

we identified a putative E2F-binding motif, EBS1 (-3/+5; 5'-CTTGGCGC-3') using the JASPAR (<http://jaspar.genereg.net/>) and TFSEARCH databases (<http://www.cbrc.jp/research/db/TFSEARCH.html>) (Figure 2A). This putative binding site shared high similarity with the consensus motif for E2F, TTTSSCGC with S = G or C. Since E2F transcription factors are frequently deregulated in a variety of tumors, we tested the effect of E2Fs on the *DSCC1* promoter activity. Although E2F1, E2F2, E2F3, and E2F4 increased the promoter activity, E2F6 did not change the activity. E2F1, which showed the strongest induction among the four members, augmented the activity in a dose-dependent fashion (Figure 2B and S2A). This enhancement was also observed in other cell lines including LoVo, HeLa, and HEK293 (data not shown). To examine the possible involvement of EBS1 in the enhancement, we measured reporter activity using the constructs pDSCC1-10/+109 and +10/+109 in the presence or absence of E2F1 (Figure 2C). Basal reporter activities of these reporter plasmids were not significantly different in the absence of E2F1 plasmids. Deletion of EBS1 (pDSCC1+10/+109) dramatically decreased E2F1-induced reporter activity (from 20.4-fold to 3.2-fold). Unexpectedly, enhancement of reporter activity by E2F1 was still observed in +10/+109. Further deletion up to +70 of the promoter (pDSCC1+70/+109) completely diminished E2F1-induced reporter activity (Figure 2C). In agreement with this result, we found two additional presumptive EBSs, EBS2 (+31/+38; 5'-CTTCCGGC-3') and EBS3 (+57/+64; 5'-TTGCCCGC-3') in the region between +10 and +70. To address responsibilities of EBS1, EBS2, and EBS3 for the induction, we prepared four mutant reporter constructs (Figure 2D) by substituting the GC-rich segment in E2F consensus motifs, TTTSSCGC (S = C or G) or STTTS, because these core motifs were reportedly crucial for E2F binding [13,14]. Compared with wild type pDSCC1-10/+109 (14.8-fold induction), both types of EBS1-mutant plasmids (pDSCC1-10/+109 mut1, and mut1') remarkably decreased the reporter activity in response to E2F1 (5.2-fold and 5.8-fold, respectively). Mutations in both EBS1 and EBS2 (pDSCC1-10/+109 mut1+2) further decreased in the E2F1-induced activity (3.7-fold). Mutant reporter plasmid containing substitutions in the three elements (pDSCC1-10/+109 mut1+2+3) almost diminished the enhancement (1.7-fold), suggesting that the three E2F binding motifs are responsible for the regulation of *DSCC1* promoter activity.

Interaction of E2F1 with the *DSCC1* promoter region

To determine whether E2F1 binds to the promoter region of *DSCC1*, we performed quantitative ChIP assay using anti-E2F1 antibody and a set of primers encompassing the three putative E2F-binding elements. The promoter of cell division cycle 2 gene (*CDC2*), a well-known E2F1 target, was enriched 13.4-fold with the immunoprecipitated DNA (Figure S2B). Expectedly, the *DSCC1* promoter region was enriched by up to 15.4-fold in the DNA, suggesting an interaction of the *DSCC1* promoter region with E2F1 (Figure 2E).

To confirm the involvement of E2F1 in regulating *DSCC1* expression, we investigated the silencing effect of E2F1 on *DSCC1* expression. Real-time PCR and western blot analyses showed that depletion of E2F1 decreased *DSCC1* expression (Figure 2F and S2C). RNAi-mediated knockdown of E2F1 activity was confirmed by reporter assay showing significant reduction of the *DSCC1* promoter activity from 10.4 (Ctrl siRNA) to 4.7-fold by E2F1 siRNA in SW480 cells (Figure 2G). These results suggested that *DSCC1* transcription is, at least in part, regulated by E2F1 in CRC through its interaction with the *DSCC1* promoter region, and that the three EBSs play an important role in the transcriptional

activation. To further investigate whether *DSCC1* expression is modulated by E2F transcriptional activity, we compared the relative expression of *DSCC1* with *CDK1* (*CDC2*), as readout of E2F transcriptional activity, using two independent data sets (EMEXP-3715 and GEOD-23878) in the Gene Expression Atlas database (<http://www.ebi.ac.uk/gxa/>). In the data sets, *DSCC1* and *CDK1* were significantly up-regulated in colorectal tumors compared with normal colonic tissues (Figure 3). Notably, both data sets calculated high values of correlation coefficient (EMEXP-3715, $r=0.912$ and GEOD-23878, $r=0.864$) between *DSCC1* and *CDK1*, supporting the view that *DSCC1* is another downstream gene regulated by E2F.

Effect of *DSCC1* on the proliferation of CRC cells

To address the role of its elevated expression in CRC cells, we investigated whether *DSCC1* is involved in the proliferation of cancer cells. We carried out cell viability assay using plasmids expressing both *DSCC1* shRNA (shDSCC1#1, or shDSCC1#2) and neomycin resistant gene. Plasmids containing the scrambled sequence of *DSCC1* shRNAs (shDSCC1#1scr and shDSCC1#2scr) and plasmid containing EGFP shRNA (shEGFP) served as controls. Transfection with these *DSCC1* shRNAs (shDSCC1#1, or shDSCC1#2) reduced the expression of *DSCC1*, whereas transfection with controls (shEGFP, shDSCC1#1scr and shDSCC1#2scr) had no effect (Figure 4A). HCT116 cells were cultured in media containing appropriate concentration of G418 and the cell viability was measured. We found that the number of viable cells transfected with *DSCC1*#1 or *DSCC1*#2 shRNA was significantly decreased compared to those transfected with EGFP, *DSCC1*#1scr, or *DSCC1*#2scr shRNA, indicating that *DSCC1* plays a role in the viability of cancer cells (Figure 4B). Consistent data was obtained in SW480 and RKO cells (Figure S3A). These results were confirmed in repeated experiments.

In addition, we established SW480 cells that constitutively express exogenous *DSCC1*, and compared their proliferation with control cells transfected with mock vector (Figure 4C). Consistent with the *DSCC1*-knockdown data, cells expressing exogenous *DSCC1* showed augmented cell proliferation compared to parental SW480 cells or control cells ($p=2.2\times 10^{-5}$). Similarly, exogenous *DSCC1*-expression enhanced the proliferation of HCT116 cells (Figure S3B).

Role of *DSCC1* in the induction of apoptosis

Since E2F1 conferred resistance to genotoxic insults [15,16,17], we further investigated whether elevated *DSCC1* expression plays a role in the sensitivity of cancer cells to genotoxic stimuli. SW480 cells-expressing exogenous *DSCC1* (SW480-*DSCC1*#1, #3, and #8) were exposed to γ -irradiation, and induction of apoptosis was analyzed by immunoblotting with anti-cleaved PARP antibody. As shown in Figure 5A, quantification of cleaved PARP-specific bands revealed that γ -irradiation led to 3.9, 2.6, and 1.2-fold increase of cleaved PARP in control cells (SW480-Mock#1, #3, and #4, respectively). On the other hand, 1.0, 1.4, and 1.2-fold increase was observed in response to γ -irradiation in SW480-*DSCC1*#1, #3, and #8 cells, respectively, suggesting that *DSCC1* suppressed apoptosis by γ -irradiation. In addition, treatment with camptothecin, an inhibitor of topoisomerase I, induced early apoptotic cells (annexin V-positive and PI-low) by $5.6\pm 2.9\%$ in control cells (Figure 5B), while the treatment increased early apoptotic cells by only $0.7\pm 0.3\%$ in SW480-*DSCC1* cells, indicating a significant suppression of apoptosis ($p=0.02$). These data suggested that elevated *DSCC1* expression might confer resistance to apoptotic stimuli in cancer cells. In

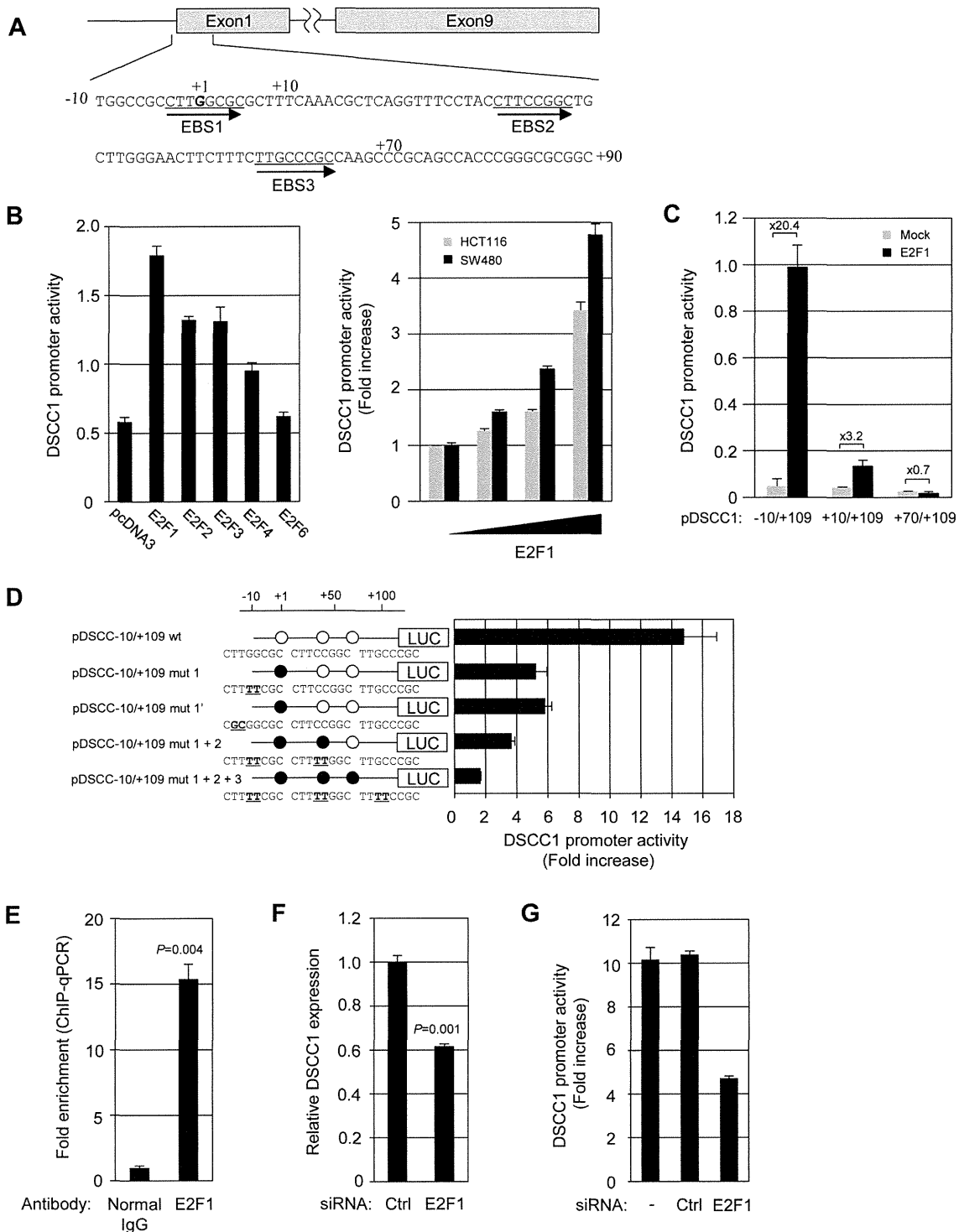


Figure 2. Regulation of *DSCC1* promoter activity by E2F transcription factor. (A) Nucleotide sequence of the -10 to +90 bp region human *DSCC1*. Three putative E2F binding motifs are underlined. (B) pDSCC1-1023/+109 was transiently transfected with pRL-TK and pcDNA3 HA-E2Fs into SW480, or with pRL-TK and pcDNA3 HA-E2F1 (0.01-1 μ g) into SW480 and HCT116 cells. (C) pDSCC1-10/+109 or the shorter promoter constructs was transfected with E2F1 or the empty vector into SW480 cells. (D) Site-directed mutation analysis of putative E2F binding sites in the proximal promoter region. pDSCC1-10/+109 or its mutant clones was transfected with E2F1 or the empty vector into SW480 cells. The data represents mean \pm SD from three independent experiments. Promoter activity indicates the relative luciferase unit or the fold induction over empty vector transfectant. (E) Chromatin immunoprecipitation was performed using anti-E2F1 antibody. The precipitated DNAs were subjected to the amplification of *DSCC1*

promoter by quantitative PCR. To ascertain the specific binding to the EBS, the amplification of a distal upstream region in the *DSCC1* promoter was used for normalization. A significant difference was determined by t-test. (F) HCT116 cells were transfected with control or E2F1 siRNA (25 nM) for 48 h. *DSCC1* expression was detected by quantitative PCR. A significant difference was determined by t-test. (G) SW480 cells were transfected with control or E2F1 siRNA (25 nM), followed 8 h later by transfection with reporter plasmid (pDSCC1-10/+109) and E2F1 expression vector or the empty vector. After 48 h, luciferase activity was measured. The data represents mean \pm SD from three independent experiments. doi:10.1371/journal.pone.0085750.g002

complete agreement with these results, knockdown of *DSCC1* potentiated camptothecin- and γ -irradiation-induced apoptosis in HCT116 cells (Figure 5C and S3C). To address whether *DSCC1* expression affects cell death induced by other types of cytotoxic reagents, we treated HCT116 cells with doxorubicin, a DNA intercalator, or MG132, a proteasome inhibitor, and measured the cleavage of PARP and caspase-3, indicators of apoptosis. Suppression of *DSCC1* augmented the cleavage of PARP and caspase-3 in response to doxorubicin, whereas knockdown of *DSCC1* did not increase the cleavage in response to MG132 (Figure S3D and S3E). Therefore, *DSCC1* may be associated with the cell death caused by DNA-damage, but not with the death by other types of cytotoxic insults. Of note, *DSCC1* depletion also enhanced induction of apoptosis by γ -irradiation in p53-null HCT116 cells (Figure S3F), suggesting that *DSCC1*-mediated resistance against apoptosis was independent of p53. These results

imply that suppression of *DSCC1* may be useful for the treatment and/or chemosensitization of CRC cells.

Discussion

Regulated by the retinoblastoma tumor suppressor, pRB, and/or related proteins, E2Fs play crucial roles in cell cycle, nucleotide synthesis, DNA replication, DNA repair, and apoptosis [18,19]. Activities of E2Fs are regulated by integration of signals transduced from the cellular DNA and the external environment. E2F1 is thought to act as an oncogene and a tumor suppressor, with its action dependent on the cellular context. Indeed, overexpression of E2F1 is observed in CRC cells, suggesting its tumorigenic role in the cancer [20]. E2F1 expression is elevated in lung metastasis of colon cancer, and correlates with thymidylate synthase expression, resulting in chemoresistance [21]. On the other hand, E2F1 is over-expressed in colon tumors with increased apoptosis and low proliferation [22]. Therefore, clarification of E2F1 targets should give a clue how this versatile transcription factor family is involved in colorectal carcinogenesis. We have demonstrated here that *DSCC1* is frequently up-regulated in CRCs through the transactivation by the E2F family of transcription factors. Although *DSCC1* is located at chromosomal region 8q, which is one of the most frequently amplified chromosomal regions in colorectal tumors [23], copy number gain or amplification was not involved in *DSCC1* up-regulation. Instead, we showed here that the flanking region of *DSCC1* transcription start site containing three E2F regulatory sites (EBS1, 2, and 3) plays a role in the transcriptional activation. A previous genome-wide ChIP-chip analysis reported that 20,000–30,000 E2F1-binding sites are distributed over the human genome, of which 51% overlapped transcription start sites [24]. The localization of EBS1, 2, and 3 is compatible with their findings. Among the three sites, EBS1 and EBS3 contain identical sequence with the core E2F1-binding motif (C/GC/GCGC), but EBS2 contains a 1-bp mismatch to the motif. Comparison of human and mouse *DSCC1* 5'-flanking sequences determined that EBS1, located at the -3 to $+5$ bp region, was well-conserved between the two species (Figure S4A). Consistent with these data, the mutation in EBS1 most remarkably reduced the E2F1-induced promoter activity among the three. Regarding other regulatory elements, we identified a region between -40 and -20 that was associated with basal promoter activity of *DSCC1* (Figure S4B). A search of transcription factor-binding elements in this region found a GC box encompassing a putative ELK1-binding site, but our reporter assay did not show significant change of the promoter activity by ELK1 (data not shown), suggesting that ELK1 may not be involved in the regulation of *DSCC1*.

Eight members of the mammalian E2F family have been recognized and characterized. Among these members, E2F1, E2F2, and E2F3 are categorized as transcriptional activators, and E2F4, E2F5, E2F6, E2F7, and E2F8 are categorized as repressors [25,26]. In our promoter assay, E2F1, E2F2, E2F3, and E2F4 induced *DSCC1* promoter activity, but E2F6 did not, showing an inconsistent result with E2F4 in the transcription. Molecular studies have uncovered that E2Fs target genes are regulated not only by their binding to DNA element(s) but also by their interacting proteins such as Rb, p107, p130, polycomb group

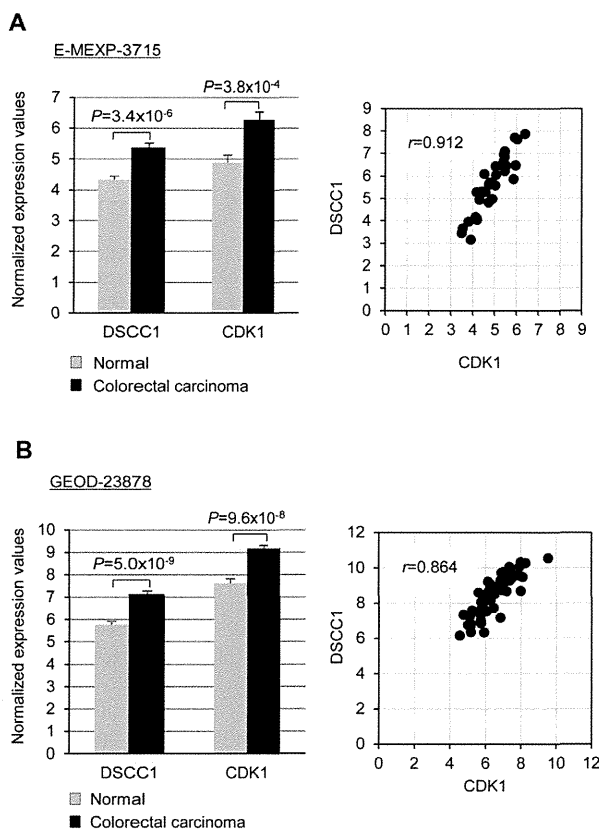


Figure 3. Positive correlation between *DSCC1* and *CDK1* expression in colorectal tumors. This association was shown by two sets of microarray data, E-MEXP-3715 (A) and GEOD-23878 (B), in the Gene Expression Atlas database (<http://www.ebi.ac.uk/gxa/>). The Pearson's correlation coefficient (r) between *DSCC1* and *CDK1* expression values was then calculated to assess their correlation. doi:10.1371/journal.pone.0085750.g003

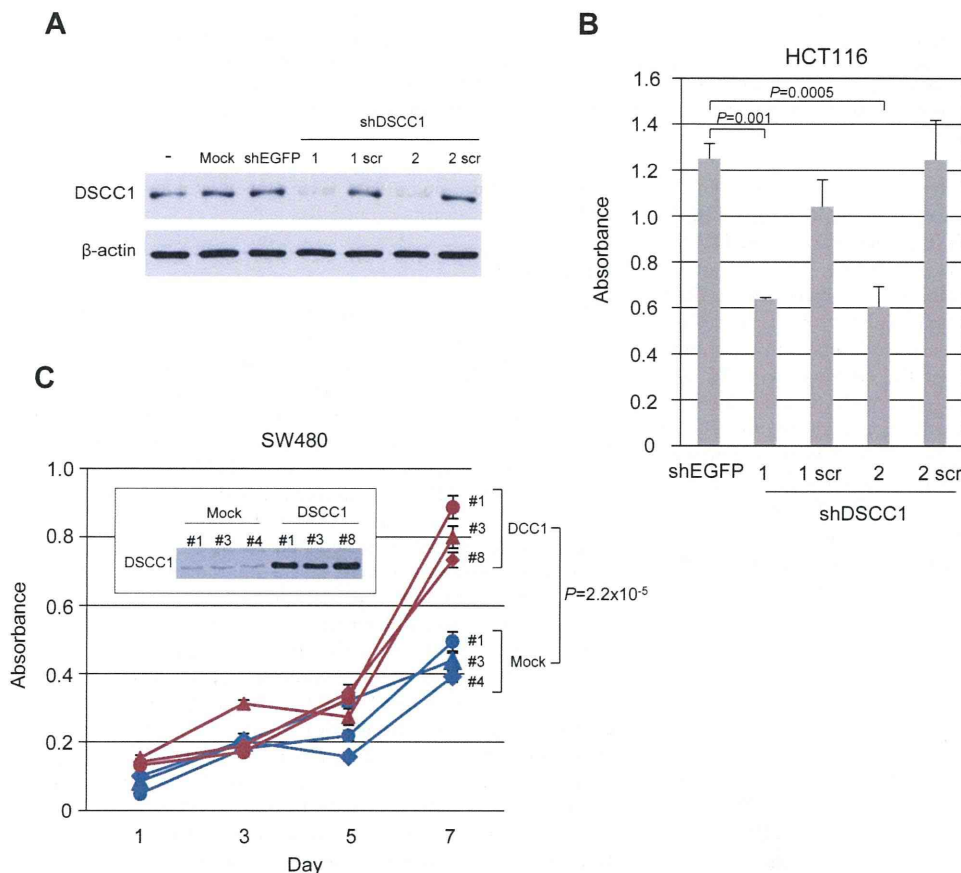


Figure 4. Involvement of DSCC1 in CRC cell proliferation. (A) HCT116 cells were transfected with control (Mock and EGFP) and DSCC1 shRNAs for 48 h using Nucleofector kit, and western blot analysis was performed. Expression of β -actin served as a control. (B) Viability of cells transfected with shRNAs was measured by WST-8 assay. The data represents mean \pm SD from three independent transfections. P values were calculated with the Dunnett's test for multiple comparisons to shEGFP-transfected cells. (C) Overexpression of DSCC1 in SW480 cells was confirmed by western blotting using anti-DSCC1 antibody. Equivalent number of three mock and three DSCC1 cells was plated in 96-well plates, and cell proliferation assays were performed at the indicated time points. The data represents mean \pm SD from five experiments. A significant difference between mock and DSCC1 cells was determined by two-way repeated measures ANOVA. doi:10.1371/journal.pone.0085750.g004

proteins, and histone-modification enzymes. Therefore, other factor(s) might affect the elevated promoter activity by E2F4. Although the direct association of E2Fs and their cofactors with the three binding sites needs future detailed analysis, the region containing the three should play a vital role in the elevated expression of DSCC1.

We here showed for the first time that DSCC1 plays an important role in survival of human cancer cells, since enhanced expression of DSCC1 induced survival of cancer cells in response to γ -irradiation, topoisomerase I inhibitor, and DNA-intercalator. The data are consistent with the finding that *Dsccl* mutants exhibit sensitivity to γ -irradiation in *Saccharomyces cerevisiae* [27,28]. Another study showed that repair of a topoisomerase I inhibitor-induced DNA double-strand breaks, required components of chromatid cohesion including *Csm3*, *Tof1*, *Mrc1*, and *Dsccl* [29]. Alternatively, DSCC1 may enhance the recombination repair through the CTF18-RFC complex. Our study additionally showed that this resistance seems to be independent of p53 because the induction of apoptosis was also potentiated in HCT116 p53^{-/-} cells (Figure S3F). Associated with CTF8, DSCC1 forms an alternate RFC with CTF18, and further stabilizes 7-subunit

complex with RFC2, RFC3, RFC4, and RFC5. Depletion of DSCC1 reduces expression of CTF18, induces decreased replication fork, increases collapse, and suppresses recovery of forks to replication inhibitors, suggesting that DSCC1 is important for DNA replication and recovery from genotoxic insults [30].

Global gene-gene interaction studies have helped gain insights into the complex genetic networks in the yeast. These studies disclosed synthetic lethal combinations of genetic dysfunction, where two genetic variations that have individually no effect on cell viability cause cell death if combined. The concept of synthetic lethality is of great importance in creating therapeutic approaches to selectively kill cancer cells, because genetic and/or epigenetic alterations are expected in cancer cells but not in noncancerous cells. For example, PARP inhibitors have been shown to induce synthetic lethality to cancer cells with BRCA1 or BRCA2 mutations [31,32]. Of note, McLellan and colleagues validated genetic interactions of synthetic lethality in the yeast between *ctf8*, *ctf18*, *dsccl*, *ctf4*, and *rad27* with genes required for the maintenance of chromosomal stability [6]. They additionally showed that these genetic interactions are conserved in *Caenorhabditis elegans*, suggesting the potential utility of these genes for the

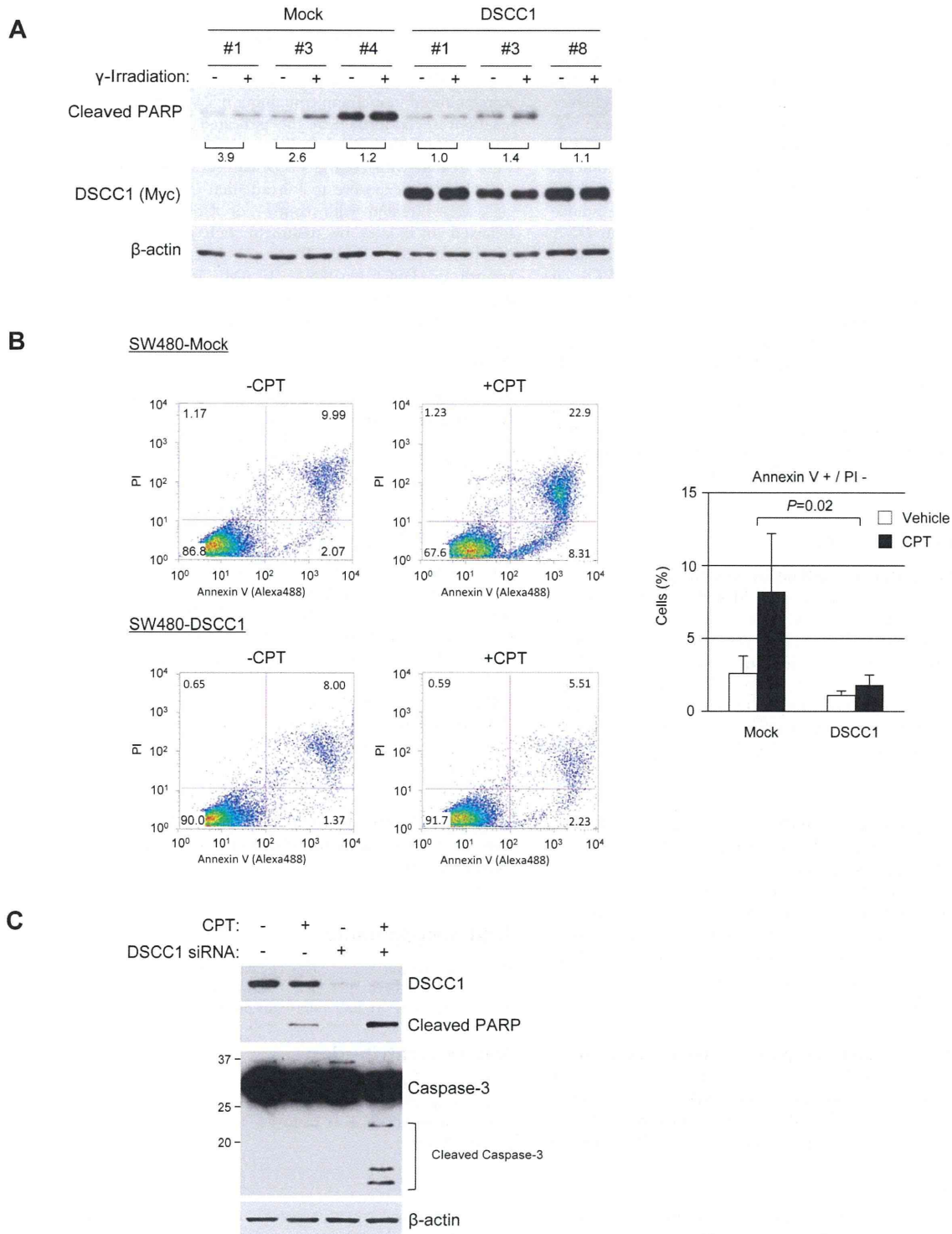


Figure 5. DSCC1 alters sensitivity to apoptotic stimuli. (A) SW480 cells stably expressing DSCC1 or mock (empty vector) were exposed to γ -irradiation (5 Gy). The cells were harvested 24 h after exposure, and the lysates were subjected to western blot analysis. (B) SW480 cells stably expressing DSCC1 or mock were treated with camptothecin (CPT, 30 μ M). The cells were harvested 24 h after treatment, and the cell suspensions were subjected to annexin V staining. The data represents mean \pm SD from three different clones. Increased annexin V-positive cell population by treatment with CPT was compared between control (Mock) and DSCC1-expressing cells. A significant difference was determined by t-test. (C) HCT116 cells were transfected with control or DSCC1 siRNA, and treated with CPT (30 μ M) at 48 h. The cells were harvested 24 h after the CPT-treatment, and the lysates were subjected to western blot analysis. doi:10.1371/journal.pone.0085750.g005

treatment of colorectal tumors where CIN is frequently involved in the carcinogenesis. They also showed mutations in *ctf4*, *ctf8*, *ctf18*, and *dsc1* are synthetically lethal when combined with mutations in CIN genes including *mre11*, *smc1*, *smc3*, *scc2*, and *pds1* [6]. To test whether CTF18-RFC complex may be associated with chemosensitivity, CTF18, a member of CTF18-RFC complex, was knocked down in HCT116 cells. Interestingly, silencing of CTF18 resulted in the increased cell death in response to camptothecin (Figure S4C). Although further studies on molecular mechanism(s) underlying DSCC1- as well as CTF18-mediated chemoresistance are needed, these data may imply that DSCC1 may facilitate DNA repair through homologous recombination by the regulation of this complex. If this is the case, inhibition of DSCC1 in combination with treatment inducing genotoxic insults such as camptothecin and γ -irradiation may be an effective therapeutic option. Comprehension of DNA damage, repair activities, and anti-apoptotic abilities should be needed to clarify the threshold for apoptosis in each cell.

In summary, our data may give a clue to the understanding of new molecular mechanisms underlying resistance of cancer cells against genotoxic insults, and may contribute to the development of new strategies to overcome the chemoresistance to anti-cancer drugs.

Supporting Information

Figure S1 Subcellular localization of DSCC1. (A) HCT116 and SW480 cells were treated with MG132 (10 μ M, 6 h) or cycloheximide (100 μ g/ml). The cells were harvested at the indicated time points, and the lysates were subjected to western blot analysis. (B) High magnification images of Figure 1D (\times 180). (C) HCT116 cells expressing Myc-tagged DSCC1 were probed with anti-Myc antibody followed by FITC-conjugated anti-mouse IgG secondary antibody (green). Nuclei were counter-stained with DAPI (blue). (D) The cytoplasmic and nuclear proteins were analyzed by western blotting. (TIF)

Figure S2 Regulation of DSCC1 by E2Fs. (A) HEK293T cells were transfected with pcDNA3 HA-E2F1, -E2F2, -E2F3, -E2F4, and -E2F6 for 24 h, and the lysates were subjected to western blot analysis. (B) Chromatin immunoprecipitation was performed using anti-E2F1 antibody. The precipitated DNAs were subjected to the amplification of *CDC2* promoter by quantitative PCR. (C) HeLa cells were transfected with control or E2F1 siRNA (25 nM) for 48 h. Western blot analysis was performed using the indicated antibodies. (TIF)

Figure S3 DSCC1 alters response to genotoxic insults. (A) Viability of cells transfected with shRNAs was measured by WST-8 assay. The data represents mean \pm SD from three to five independent transfections. P values were calculated with the Dunnett's test for multiple comparisons to shEGFP-transfected

cells. (B) Overexpression of DSCC1 in HCT116 cells was confirmed by western blot analysis with anti-Flag antibody. Equivalent number of two mock clones, two DSCC1 clones, and parental HCT116 cells was plated in 96-well plates, and these cells were cultured in medium containing 0.5% FBS. Cell proliferation assays were performed at the indicated time points. The data represents mean \pm SD from eight experiments. (C) HCT116 cells were treated with control or DSCC1 siRNA (10 nM), followed 48 h later by exposure to γ -irradiation (5 Gy). (D, E) HCT116 cells were treated with control or DSCC1 siRNA (10 nM), followed 48 h later by treatment with doxorubicin (5 μ M) or MG132 (2 μ M). (F) HCT116 p53^{-/-} cells were treated with control or DSCC1 siRNA (10 nM), followed 48 h later by exposure to γ -irradiation (5 Gy). The cells were harvested 24 h after exposure, and the lysates were subjected to western blot analysis.

(TIF)

Figure S4 Alignment of human and mouse DSCC1 5'-flanking sequence. (A) Alignment of human and mouse *DSCC1* 5'-flanking sequence by the DBTSS database (<http://dbtss.hgc.jp/>). Top strand represents the 5'-flanking sequences of human *DSCC1*, and the bottom strand represents the 5'-flanking sequences of mouse *Dsc1*. E2F binding motifs are underlined. (B) pDSCC1-133/+109 or the shorter promoter constructs was transfected with pRL-TK into SW480 cells. The promoter activity was measured by luciferase activity. Each value represents mean \pm SD from three independent transfections. (C) The effect of CTF18 siRNA (S: 5'-CCAACUGCCUGGUCAUCG-3', AS: 5'-UCGAUGACCAGGCAGUUG-3') was evaluated by quantitative PCR (CTF18 primers, forward: 5'-CTTCTCGGTGTGGCAGGA-3', reverse: 5'-CAGCAGGAGTGTGTCAGCAG-3'). HCT116 cells were treated with control or CTF18 siRNA (10 nM), followed 48 h later by treatment with CPT (30 μ M). The cells were harvested 24 h after treatment, and the lysates were subjected to western blot analysis. (TIF)

Table S1 Correlations between DSCC1 expression and the clinicopathological characteristics of the 40 colon cancer patients. (XLS)

Acknowledgments

We thank Masashi Miura, Seira Hatakeyama, and Hiromi Toyoda (The University of Tokyo) for their technical assistance and Yumiko Ishii (IMSUT FACS Core Laboratory) for the assistance of flow cytometry.

Author Contributions

Conceived and designed the experiments: KY YF. Performed the experiments: KY NT. Analyzed the data: RY AN SI SM. Contributed reagents/materials/analysis tools: TI TF MS GT KH YN. Wrote the paper: KY YF.

References

- Rajagopalan H, Nowak MA, Vogelstein B, Lengauer C (2003) The significance of unstable chromosomes in colorectal cancer. *Nat Rev Cancer* 3: 695–701.
- Wang Z, Cummins JM, Shen D, Cahill DP, Jallepalli PV, et al. (2004) Three classes of genes mutated in colorectal cancers with chromosomal instability. *Cancer Res* 64: 2998–3001.
- Barber TD, McManus K, Yuen KW, Reis M, Parmigiani G, et al. (2008) Chromatid cohesion defects may underlie chromosome instability in human colorectal cancers. *Proc Natl Acad Sci U S A* 105: 3443–3448.
- Mayer ML, Gygi SP, Aebersold R, Hieter P (2001) Identification of RFC(Ctf18p, Ctf8p, Dcc1p): an alternative RFC complex required for sister chromatid cohesion in *S. cerevisiae*. *Mol Cell* 7: 959–970.
- Lin YM, Furukawa Y, Tsunoda T, Yue CT, Yang KC, et al. (2002) Molecular diagnosis of colorectal tumors by expression profiles of 50 genes expressed differentially in adenomas and carcinomas. *Oncogene* 21: 4120–4128.
- McLellan J, O'Neil N, Tarailo S, Stoepel J, Bryan J, et al. (2009) Synthetic lethal genetic interactions that decrease somatic cell proliferation in *Caenorhabditis elegans* identify the alternative RFC CTF18 as a candidate cancer drug target. *Mol Biol Cell* 20: 5306–5313.
- Bermudez VP, Maniwa Y, Tappin I, Ozato K, Yokomori K, et al. (2003) The alternative Ctf18-Dcc1-Ctf8-replication factor C complex required for sister chromatid cohesion loads proliferating cell nuclear antigen onto DNA. *Proc Natl Acad Sci U S A* 100: 10237–10242.

8. Pan X, Ye P, Yuan DS, Wang X, Bader JS, et al. (2006) A DNA integrity network in the yeast *Saccharomyces cerevisiae*. *Cell* 124: 1069–1081.
9. Tong AH, Lesage G, Bader GD, Ding H, Xu H, et al. (2004) Global mapping of the yeast genetic interaction network. *Science* 303: 808–813.
10. Gellon L, Razidlo DF, Gleeson O, Verra L, Schulz D, et al. (2011) New functions of Ctf18-RFC in preserving genome stability outside its role in sister chromatid cohesion. *PLoS Genet* 7: e1001298.
11. Yamaguchi K, Sakai M, Shimokawa T, Yamada Y, Nakamura Y, et al. (2010) C20orf20 (MRG-binding protein) as a potential therapeutic target for colorectal cancer. *Br J Cancer* 102: 325–331.
12. Shimokawa T, Furukawa Y, Sakai M, Li M, Miwa N, et al. (2003) Involvement of the FGF18 gene in colorectal carcinogenesis, as a novel downstream target of the beta-catenin/T-cell factor complex. *Cancer Res* 63: 6116–6120.
13. Zheng N, Fraenkel E, Pabo CO, Pavletich NP (1999) Structural basis of DNA recognition by the heterodimeric cell cycle transcription factor E2F-DP. *Genes Dev* 13: 666–674.
14. Xu X, Bieda M, Jin VX, Rabinovich A, Oberley MJ, et al. (2007) A comprehensive ChIP-chip analysis of E2F1, E2F4, and E2F6 in normal and tumor cells reveals interchangeable roles of E2F family members. *Genome Res* 17: 1550–1561.
15. Hirano G, Izumi H, Kidani A, Yasuniwa Y, Han B, et al. (2010) Enhanced expression of PCAF endows apoptosis resistance in cisplatin-resistant cells. *Mol Cancer Res* 8: 864–872.
16. Wikonkal NM, Remenyik E, Knezevic D, Zhang W, Liu M, et al. (2003) Inactivating E2f1 reverts apoptosis resistance and cancer sensitivity in Trp53-deficient mice. *Nat Cell Biol* 5: 655–660.
17. Zheng C, Ren Z, Wang H, Zhang W, Kalvakolanu DV, et al. (2009) E2F1 Induces tumor cell survival via nuclear factor-kappaB-dependent induction of EGR1 transcription in prostate cancer cells. *Cancer Res* 69: 2324–2331.
18. Nevins JR (2001) The Rb/E2F pathway and cancer. *Hum Mol Genet* 10: 699–703.
19. Wong JV, Dong P, Nevins JR, Mathey-Prevot B, You L (2011) Network calisthenics: control of E2F dynamics in cell cycle entry. *Cell Cycle* 10: 3086–3094.
20. Suzuki T, Yasui W, Yokozaki H, Naka K, Ishikawa T, et al. (1999) Expression of the E2F family in human gastrointestinal carcinomas. *International journal of cancer Journal international du cancer* 81: 535–538.
21. Banerjee D, Gorlick R, Liefshitz A, Danenberg K, Danenberg PC, et al. (2000) Levels of E2F-1 expression are higher in lung metastasis of colon cancer as compared with hepatic metastasis and correlate with levels of thymidylate synthase. *Cancer Res* 60: 2365–2367.
22. Zacharatos P, Kotsinas A, Evangelou K, Karakaidos P, Vassiliou LV, et al. (2004) Distinct expression patterns of the transcription factor E2F-1 in relation to tumour growth parameters in common human carcinomas. *J Pathol* 203: 744–753.
23. Meijer GA, Hermens MA, Baak JP, van Diest PJ, Meuwissen SG, et al. (1998) Progression from colorectal adenoma to carcinoma is associated with non-random chromosomal gains as detected by comparative genomic hybridisation. *J Clin Pathol* 51: 901–909.
24. Bieda M, Xu X, Singer MA, Green R, Farnham PJ (2006) Unbiased location analysis of E2F1-binding sites suggests a widespread role for E2F1 in the human genome. *Genome Res* 16: 595–605.
25. DeGregori J, Johnson DG (2006) Distinct and Overlapping Roles for E2F Family Members in Transcription, Proliferation and Apoptosis. *Curr Mol Med* 6: 739–748.
26. Iaquinta PJ, Lees JA (2007) Life and death decisions by the E2F transcription factors. *Curr Opin Cell Biol* 19: 649–657.
27. Bennett CB, Lewis LK, Karthikeyan G, Lobachev KS, Jin YH, et al. (2001) Genes required for ionizing radiation resistance in yeast. *Nat Genet* 29: 426–434.
28. Game JC, Williamson MS, Baccari C (2005) X-ray survival characteristics and genetic analysis for nine *Saccharomyces* deletion mutants that show altered radiation sensitivity. *Genetics* 169: 51–63.
29. Redon C, Pilch DR, Bonner WM (2006) Genetic analysis of *Saccharomyces cerevisiae* H2A serine 129 mutant suggests a functional relationship between H2A and the sister-chromatid cohesion partners Csm3-Tof1 for the repair of topoisomerase I-induced DNA damage. *Genetics* 172: 67–76.
30. Terret ME, Sherwood R, Rahman S, Qin J, Jallepalli PV (2009) Cohesin acetylation speeds the replication fork. *Nature* 462: 231–234.
31. Bryant HE, Schultz N, Thomas HD, Parker KM, Flower D, et al. (2005) Specific killing of BRCA2-deficient tumours with inhibitors of poly(ADP-ribose) polymerase. *Nature* 434: 913–917.
32. Farmer H, McCabe N, Lord CJ, Tutt AN, Johnson DA, et al. (2005) Targeting the DNA repair defect in BRCA mutant cells as a therapeutic strategy. *Nature* 434: 917–921.

Early detection of metachronous bile duct cancer in Lynch syndrome: report of a case

Kunitoshi Shigeyasu · Kohji Tanakaya · Takeshi Nagasaka · Hideki Aoki · Toshiyoshi Fujiwara · Kokichi Sugano · Hideki Ishikawa · Teruhiko Yoshida · Yoshihiro Moriya · Yoichi Furukawa · Ajay Goel · Hitoshi Takeuchi

Received: 21 October 2012 / Accepted: 3 June 2013
© The Author(s) 2013. This article is published with open access at Springerlink.com

Abstract Lynch syndrome is an autosomal dominant disease associated with a high incidence of colorectal, endometrial, stomach, ovarian, pancreatic, ureter and renal pelvis, bile duct and brain tumors. The syndrome can also include sebaceous gland adenomas and keratoacanthomas, and carcinoma of the small bowel. The lifetime risk for bile duct cancer in patients with Lynch syndrome is approximately 2 %. The present report describes a case of Lynch syndrome with metachronous bile duct cancer diagnosed at an early stage. The patient was a 73-year-old Japanese male who underwent a successful left lobectomy of the liver, and there was no sign of recurrence for 2 years postoperative. However, this patient harbored a germline

mutation in *MLH1*, which prompted diagnostic examinations for noncolorectal tumors when a periodic surveillance blood examination showed abnormal values of hepatobiliary enzymes. Although most patients with bile duct cancer are diagnosed at an advanced stage, the bile duct cancer was diagnosed at an early stage in the present patient due to the observation of the gene mutation and the preceding liver tumor. This case illustrates the importance of continuous surveillance for extracolonic tumors, including bile duct cancer, in patients with Lynch syndrome.

Keywords Lynch syndrome · Bile duct cancer · Surveillance · Early detection

K. Shigeyasu · K. Tanakaya · H. Aoki · H. Takeuchi
Department of Surgery, Iwakuni Clinical Center,
Yamaguchi, Japan

K. Shigeyasu (✉) · T. Nagasaka · T. Fujiwara
Department of Gastroenterological Surgery, Okayama
University Graduate School of Medicine, Dentistry
and Pharmaceutical Sciences, 2-5-1 Shikata-cho,
Kita-ku, Okayama, Okayama 700-8558, Japan
e-mail: gmd421045@s.okayama-u.ac.jp

K. Sugano
Oncogene Research Unit Cancer Prevention Unit, Tochigi
Cancer Center Research Institute, Tochigi, Japan

H. Ishikawa · T. Yoshida · Y. Moriya · Y. Furukawa
HNPPCC Registry and Genetic Testing Project of the Japanese
Society for Cancer of the Colon and Rectum (JSCCR),
Tokyo, Japan

H. Ishikawa
Department of Molecular-Targeting Cancer Prevention, Kyoto
Prefectural University of Medicine, Osaka, Japan

T. Yoshida
Genetics Division, National Cancer Center Research Institute,
Tokyo, Japan

Y. Moriya
Department of Surgery, National Cancer Center Hospital,
Tokyo, Japan

Y. Furukawa
Division of Clinical Genome Research, Advanced Clinical
Research Center, Institute of Medical Science, The University
of Tokyo, Tokyo, Japan

A. Goel
Division of Gastroenterology, Department of Internal Medicine,
Charles A Sammons Cancer Center and Baylor Research
Institute, Baylor University Medical Center, Dallas, TX, USA

Introduction

Lynch syndrome, also known as hereditary nonpolyposis colorectal cancer (HNPCC), is an inherited autosomal dominant disorder associated with germline mutations in genes involved in DNA mismatch repair (MMR), including *MLH1*, *MSH2*, *MSH6* and *PMS2* [1]. Although variable, the lifetime risk of developing colorectal cancer (CRC) in patients with Lynch syndrome is approximately 80 %, with male carriers having a higher cumulative risk than female carriers [2]. Carriers of these mutations also have an increased lifetime risk of developing extracolonic tumors, such as endometrial, stomach, ovarian, pancreas, ureter and renal pelvis, bile duct and brain (usually glioblastoma) tumors. Further, the syndrome may also include sebaceous gland adenomas, keratoacanthomas, and carcinoma of the small bowel, although these occur at a somewhat lower incidence than the other neoplasms [3].

Since the 1980s, conventional surveillance by colonoscopy has been recommended for Lynch syndrome families. Some studies have shown that periodic examination by colonoscopy can detect CRC at an early stage, leading to a 62 % reduction in the risk of malignancy and a significant reduction in mortality associated with CRC [4–8]. While screening may be effective for the early detection of endometrial cancer in these patients [9–11], the efficacy of surveillance for other forms of co-occurring tumors has not yet been established.

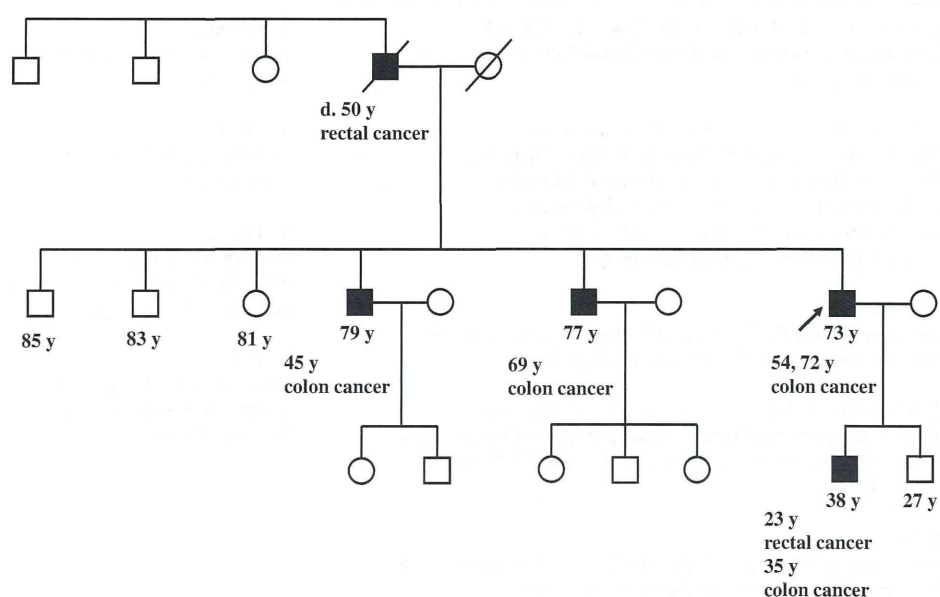
The present report describes the case of a patient with Lynch syndrome in whom bile duct cancer was detected in its early stages after abnormal hepatobiliary function was detected during routine surveillance, which prompted additional diagnostic measures.

Case presentation

A 73-year-old male with a history of synchronous and metachronous CRCs had undergone right hemicolectomy with partial liver resection at 54 years of age for synchronous ascending and transverse colonic tumors (three lesions) with a single liver metastasis (Stage IV: Union Internationale Contre le Cancer, UICC TNM staging). At 72 years, he developed metachronous sigmoid colon cancer (Stage I), which was treated by surgical resection. Although the age of CRC onset was relatively late, his family history met the revised Amsterdam criteria for the diagnosis of Lynch syndrome (Fig. 1); his father developed rectal cancer at 50 years of age, his elder brother had developed advanced CRC when he was 45, another brother developed CRC when he was 69 and one of his sons had developed metachronous CRCs at 23 and 35 years of age. After obtaining informed consent, genetic testing for MMR identified a germline mutation in *MLH1*, c.209_211delAAG. Because this deletion is localized near the 5' site of exon 3, a reverse transcriptase polymerase chain reaction (RT-PCR) analysis was performed and revealed exon 3 (279 bp) skipping. Thereafter, the patient was enrolled in a surveillance program for Lynch syndrome (colonoscopy, gastroduodenoscopy, abdominal ultrasound, urinalysis and urine cytology every year) with a routine postsurgical examination protocol (periodic abdominal ultrasonography and computed tomography every 6 months and blood examinations every 3 months).

One year after the surgical resection for Stage I sigmoid colon cancer, a periodic examination revealed increased values of hepatobiliary enzymes in his peripheral blood sample, with aspartate aminotransferase of 53 U/L (normal range 13–33 U/L), alanine aminotransferase of 109 U/L

Fig. 1 The patient's pedigree. The patient's family satisfied the revised Amsterdam criteria for the diagnosis of Lynch syndrome



(normal range 6–27 U/L) and alkaline phosphatase of 635 U/L (normal range 115–359 U/L). His total bilirubin level was also slightly elevated at 1.6 mg/dL (normal range 0.3–1.28 mg/dL) (Table 1). Further examinations were performed to screen for Lynch syndrome-related tumors. Abdominal ultrasonography revealed dilatation of the left intrahepatic bile duct. Computed tomography and endoscopic retrograde cholangiography revealed a tumor in the left hepatic bile duct and dilatation of the left intrahepatic bile duct, respectively (Fig. 2). He underwent surgical resection for a presumed diagnosis of bile duct cancer.

Intraoperative cholangioscopy detected a papillary tumor at the origin of the left hepatic duct. A histological examination confirmed a well-differentiated papillary adenocarcinoma of the bile duct [T1 (fibromuscular layer,

fm) N0M0 Stage IA (UICC TNM staging)]. As expected, immunohistochemical staining demonstrated that the tumor was MLH1 negative and MSH2 positive (Fig. 3), which was in agreement with the germline mutation in *MLH1*. A microsatellite instability (MSI) analysis diagnosed the tumor as MSI high using the National Cancer Institute panel (NCI panel: D2S123, D5S346, D17S250, BAT25 and BAT26); replication errors were observed in four microsatellite markers [MSI-H (4/5)] (Fig. 4).

Discussion

The Bethesda guidelines, proposed in 1996 and revised in 2002, are probably the most important clinical guidelines

Table 1 Laboratory data

Parameters	Normal range	Units	3 months before operation	Just before operation	3 months after operation
Total bilirubin	0.3–1.28	mg/dl	1.2	1.6	1.2
Aspartate aminotransferase	13–33	U/L	31	53	19
Alanine aminotransferase	6–27	U/L	48	109	16
Alkaline phosphatase	115–359	U/L	ND	635	347

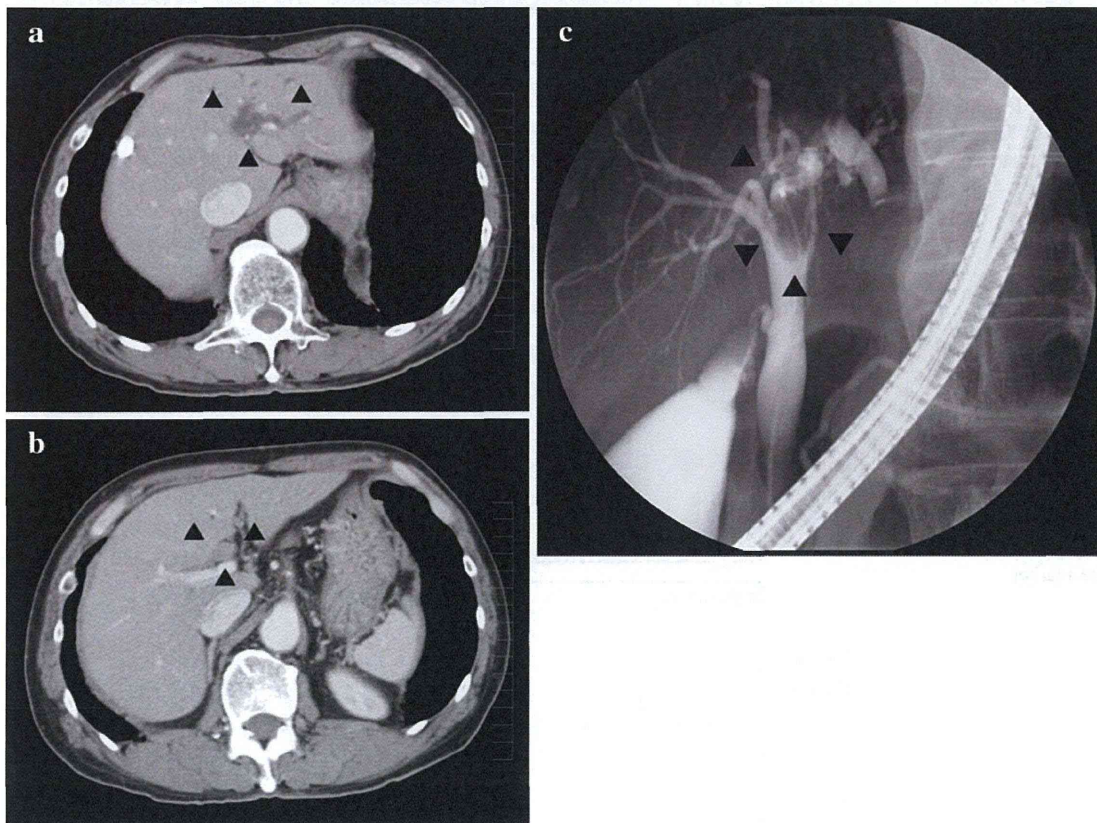


Fig. 2 Imaging of the hepatobiliary system. Computed tomography (a, b) and endoscopic retrograde cholangiography (c) revealed a mass in the left hepatic bile duct and a dilated left intrahepatic bile duct (arrowheads)

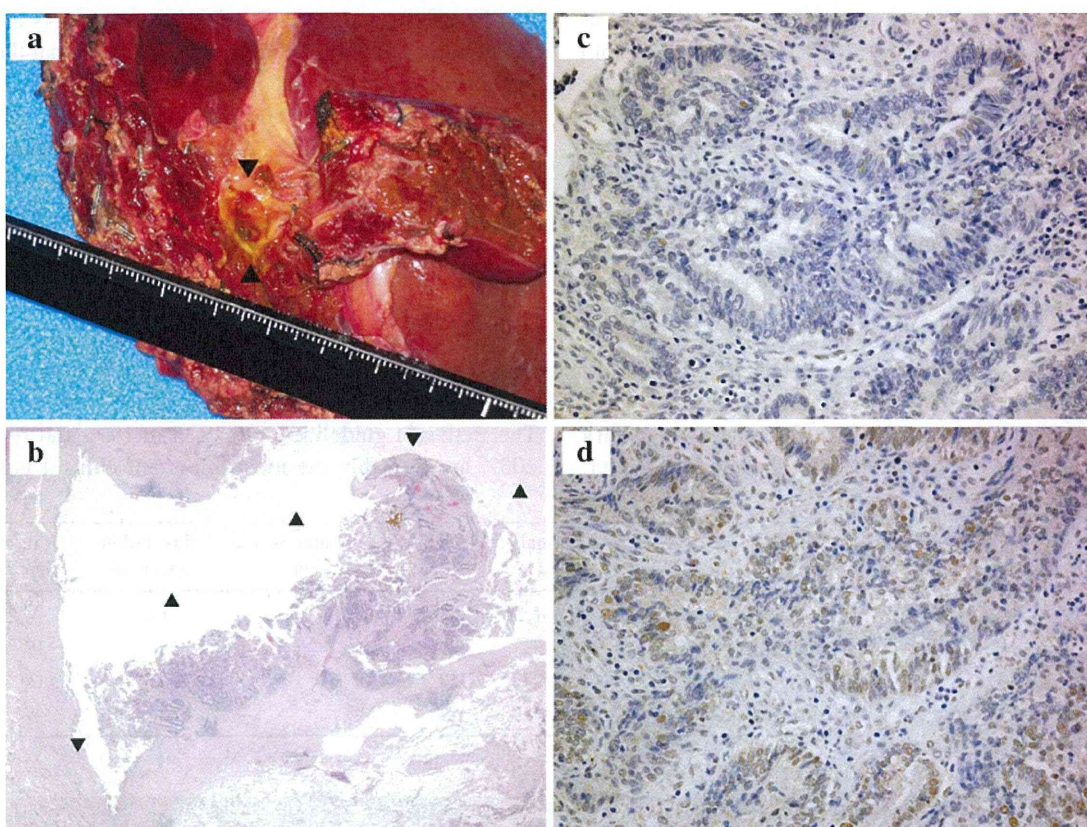
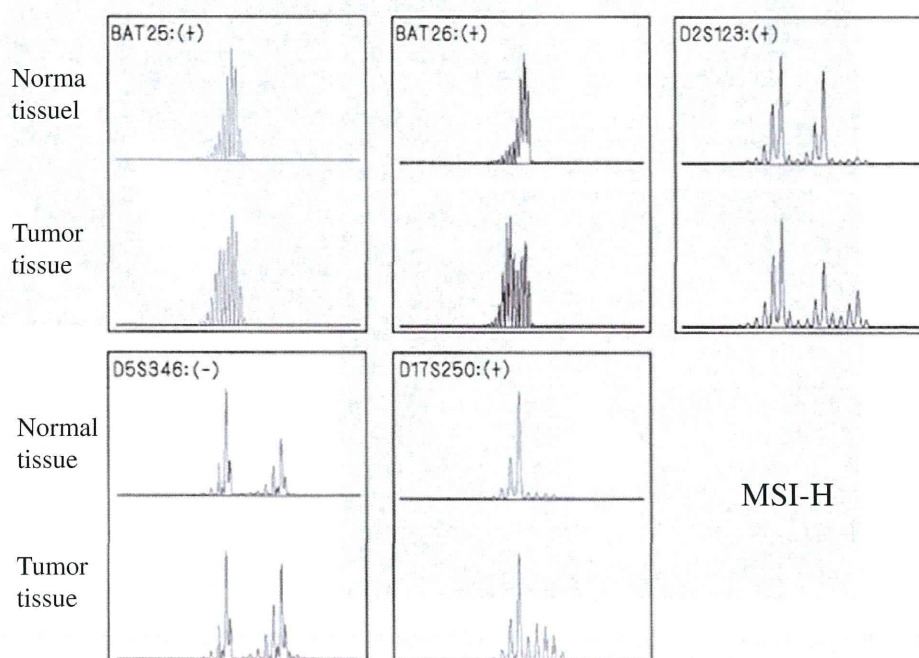


Fig. 3 The results of a histopathological analysis of the tumor sample obtained from the left lobectomy. **a** The gross appearance of the resected tissue. **b** The H&E staining ($\times 100$) revealed a well-differentiated papillary hilar bile duct cancer [T1 (fibromuscular

layer, fm) N0M0 Stage IA (Union Internationale Contre le Cancer, UICC TNM staging) (*arrowheads*). **c** Immunostaining of the tumor for MLH1 ($\times 400$). **d** Immunostaining of the tumor for MSH2 ($\times 400$). Immunoreactivity was observed for MSH2, but not for MLH1

Fig. 4 The results of a microsatellite instability (MSI) analysis. The microsatellite instability (MSI) analysis showed that the tumor was MSI high according to the National Cancer Institute panel (NCI panel: D2S123, D5S346, D17S250, BAT25, and BAT26); replication errors were observed in four microsatellite markers [MSI-H (4/5)]. +, -: Existence of replication errors in each microsatellite marker



for Lynch syndrome, and include Lynch syndrome-associated tumors, such as colorectal, endometrial, stomach, ovarian, pancreas, ureter and renal pelvis, bile duct and brain tumors, as well as sebaceous gland adenomas, keratoacanthomas and carcinoma of the small bowel [3]. The lifetime risk for biliary tract cancer in patients with Lynch syndrome is approximately 2 % [2]. Mecklin et al. [12] described 11 cases of bile duct cancer in Lynch syndrome families; the mean age at diagnosis was 56.9 years. Of these 11 cases, seven tumors arose in the common bile duct, whereas four originated in the intrahepatic bile duct.

The International Society for Gastrointestinal Hereditary Tumors database (InSiGHT/LOVD database; <http://www.insight-group.org/mutations/>) contains two cases of bile duct cancer with a germline mutation in *MLH1* (deletion in exon 16, c.1732-?_1896+?del). In our case, the patient harbored a germline mutation in *MLH1* c.209_211delAAG, which resulted in exon 3 skipping (Fig. 5). Of note, this mutation has not been reported previously, although one report showed that a similar deletion of *MLH1*, c.210_213delAGAA, also leads to exon 3 skipping [13].

CRC is the most common Lynch syndrome-related tumor, with a lifetime risk of approximately 80 %. Early-stage CRC is detectable by surveillance of the colorectum, and early treatment can decrease mortality. Endometrial cancer is the next most common Lynch syndrome-related

cancer, with a lifetime risk of 20–60 %, and conventional screening is useful for the early detection of this cancer [2]. Thus, established surveillance protocols are effective tools for the early detection of CRC and endometrial cancer [4–11]. In contrast, the lifetime risk of bile duct cancer in patients with Lynch syndrome is only 2 % [2]. Surveillance for bile duct cancer is not recommended for Lynch syndrome families, because there are no established strategies for the early detection of bile duct cancer. The routine surveillance protocol for Lynch syndrome in our hospital is almost the same as that recommended by the Lynch syndrome surveillance program (i.e., colonoscopy, gynecological examination, transvaginal ultrasound, aspiration biopsy, gastroduodenoscopy, abdominal ultrasound, urinalysis and urine cytology every year) reported by Vasen et al. [2]. These examinations are not specifically targeted toward early detection of bile duct cancer. However, in the surveillance of patients with Lynch syndrome and their relatives, it is important to consider the risks of developing bile duct cancer, which is higher in these patients than in the general population. Carriers of MMR gene mutations are at an elevated risk of bile duct cancer compared with the general population (standardized incidence ratio 5.94) [14, 15]. Most cases of bile duct cancers, which can rapidly progress to an advanced stage because of the lack of muscularis mucosae in the wall of the bile duct, are typically diagnosed at advanced stages and are therefore associated with much higher mortality rates than cancers that occur outside the hepatobiliary system [16].

The early detection of bile duct cancer is challenging. The most promising, noninvasive and cost-effective tools include blood examinations and abdominal ultrasonography. Blood examinations can reveal increased values of hepatobiliary enzymes in 75 % of bile duct cancer patients without jaundice [17] [18], and abdominal ultrasonography can improve the early detection rates of bile duct cancer [19]. Although blood examinations and abdominal ultrasonography are useful for detecting abdominal disease, including bile duct cancer, these modalities are not utilized frequently in the surveillance program for patients with Lynch syndrome.

In the present case, a routine postsurgical examination protocol (i.e., periodic abdominal ultrasonography and computed tomography every 6 months and blood examination every 3 months) was conducted. We consider the bile duct cancer as a Lynch syndrome-related tumor. Therefore, we immediately began diagnostic investigations for bile duct cancer when the surveillance blood examination results showed abnormal hepatobiliary function. In contrast, we would not have been able to detect the bile duct cancer at an early stage in this patient had we relied on only a traditional surveillance program for Lynch syndrome instead of our

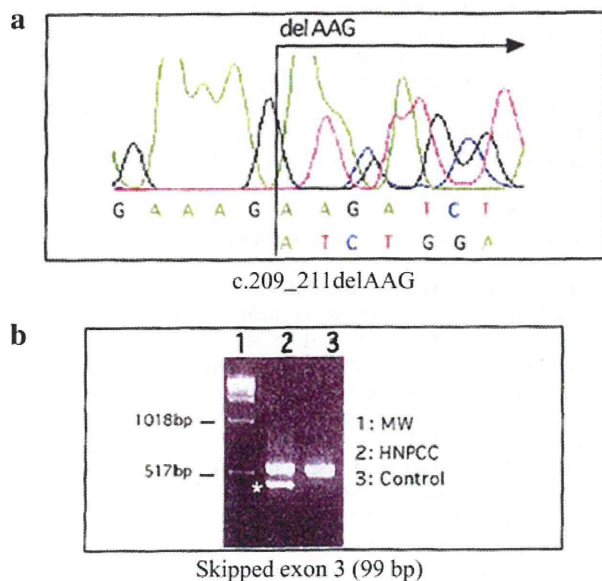


Fig. 5 The results of the genetic analysis of *MLH1*. **a** Direct sequencing of *MLH1* revealed that the patient harbored a germline mutation in *MLH1*, c.209_211delAAG, which resulted in exon 3 skipping. **b** Reverse transcriptase polymerase chain reaction (RT-PCR) of *MLH1* messenger RNA (mRNA) revealed a shorter product [skipping of exon 3 (99 bp)] in the present case (lane 2 HNPCC). MW denotes the molecular weight marker. Control denotes the RT-PCR product obtained from normal *MLH1* mRNA

routine postsurgical examination protocol, because frequent blood examinations and abdominal ultrasonography are not included as part of the surveillance protocol for Lynch syndrome.

The present case suggests that the combination of periodic blood examinations and abdominal ultrasonography every 3–6 months may be useful for the early detection of bile duct cancer in patients with Lynch syndrome. In the present case, the patient received a successful early diagnosis and treatment of rare bile duct cancer as a result of a blood examination in the postsurgical state. Although blood examinations are not part of a routine postsurgical examination protocol for Lynch syndrome patients, as this case shows, they may be effective, and should be considered for inclusion in the surveillance for Lynch syndrome. In addition, abdominal ultrasonography is noninvasive and can visualize dilated bile ducts that are often present in patients with early bile duct cancer. Further research is needed to draw definitive conclusions regarding the utility of periodic blood examinations and abdominal ultrasonography in this context, but our present case indicates that such examinations are warranted.

Conclusion

The present report described the case of a patient with Lynch syndrome in whom bile duct cancer was detected in its early stages after a periodic blood examination showed abnormal liver function. The assessment of the hepatobiliary enzymes and subsequent ultrasonography and computed tomography facilitated early detection of this cancer. Although most cases of bile duct cancer are diagnosed at advanced stages, the fact that this patient had a known germline mutation in *MLH1* resulted in a higher level of suspicion regarding noncolorectal tumors, which prompted the use of additional diagnostic investigations for such tumors when his ordinary blood examination suggested abnormal hepatobiliary function. This case illustrates the importance of surveillance for noncolorectal tumors in patients with Lynch syndrome. Physicians should be aware that patients with Lynch syndrome are at a higher risk of developing rare extracolonic cancers compared with the general population. Since these cancers are associated with a poor prognosis, early detection through surveillance may improve the outcomes in these patients. We conclude that the combination of periodic blood examinations and abdominal ultrasonography every 3–6 months may be useful for the early detection of bile duct cancer in Lynch syndrome patients.

Acknowledgments This work was supported in part by Grants-in-Aid for Cancer Research G21S-9-2 (to Kokichi Sugano).

Conflict of interest The authors have no conflicts of interest.

Open Access This article is distributed under the terms of the Creative Commons Attribution License which permits any use, distribution, and reproduction in any medium, provided the original author(s) and the source are credited.

References

1. Lynch HT, de la Chapelle A. Hereditary colorectal cancer. *N Engl J Med*. 2003;348:919–32.
2. Vasen HF, Moslein G, Alonso A, Bernstein I, Bertario L, Blanco I, et al. Guidelines for the clinical management of Lynch syndrome (hereditary non-polyposis cancer). *J Med Genet*. 2007;44:353–62.
3. Umar A, Boland CR, Terdiman JP, Syngal S, de la Chapelle A, Ruschoff J, et al. Revised Bethesda Guidelines for hereditary nonpolyposis colorectal cancer (Lynch syndrome) and microsatellite instability. *J Natl Cancer Inst*. 2004;96:261–8.
4. Jarvinen HJ, Aarnio M, Mustonen H, Aktan-Collan K, Aaltonen LA, Peltomaki P, et al. Controlled 15-year trial on screening for colorectal cancer in families with hereditary nonpolyposis colorectal cancer. *Gastroenterology*. 2000;118:829–34.
5. Renkonen-Sinisalo L, Aarnio M, Mecklin JP, Jarvinen HJ. Surveillance improves survival of colorectal cancer in patients with hereditary nonpolyposis colorectal cancer. *Cancer Detect Prev*. 2000;24:137–42.
6. Arrigoni A, Sprujevnik T, Alvisi V, Rossi A, Ricci G, Pennazio M, et al. Clinical identification and long-term surveillance of 22 hereditary non-polyposis colon cancer Italian families. *Eur J Gastroenterol Hepatol*. 2005;17:213–9.
7. de Vos tot Nederveen Cappel WH, Nagengast FM, Griffioen G, Menko FH, Taal BG, Kleibeuker JH, et al. Surveillance for hereditary nonpolyposis colorectal cancer: a long-term study on 114 families. *Dis Colon Rectum*. 2002;45:1588–94.
8. de Jong AE, Hendriks YM, Kleibeuker JH, de Boer SY, Cats A, Griffioen G, et al. Decrease in mortality in Lynch syndrome families because of surveillance. *Gastroenterology*. 2006;130:665–71.
9. Dove-Edwin I, Boks D, Goff S, Kenter GG, Carpenter R, Vasen HF, et al. The outcome of endometrial carcinoma surveillance by ultrasound scan in women at risk of hereditary nonpolyposis colorectal carcinoma and familial colorectal carcinoma. *Cancer*. 2002;94:1708–12.
10. Rijcken FE, Mourits MJ, Kleibeuker JH, Hollema H, van der Zee AG. Gynecologic screening in hereditary nonpolyposis colorectal cancer. *Gynecol Oncol*. 2003;91:74–80.
11. Renkonen-Sinisalo L, Butzow R, Leminen A, Lehtovirta P, Mecklin JP, Jarvinen HJ. Surveillance for endometrial cancer in hereditary nonpolyposis colorectal cancer syndrome. *Int J Cancer*. 2007;120:821–4.
12. Mecklin JP, Jarvinen HJ, Virolainen M. The association between cholangiocarcinoma and hereditary nonpolyposis colorectal carcinoma. *Cancer*. 1992;69:1112–4.
13. Renkonen E, Lohi H, Jarvinen HJ, Mecklin JP, Peltomaki P. Novel splicing associations of hereditary colon cancer related DNA mismatch repair gene mutations. *J Med Genet*. 2004;41:e95.
14. Win AK, Lindor NM, Young JP, Macrae FA, Young GP, Williamson E, et al. Risks of primary extracolonic cancers following colorectal cancer in Lynch syndrome. *J Natl Cancer Inst*. 2012. doi:10.1093/jnci/djs351.
15. Geary J, Sasiemi P, Houlston R, Izatt L, Eeles R, Payne SJ, et al. Gene-related cancer spectrum in families with hereditary non-polyposis colorectal cancer (HNPCC). *Fam Cancer*. 2008;7:163–72.

16. Sai JK, Suyama M, Kubokawa Y, Watanabe S, Maehara T. Early detection of extrahepatic bile-duct carcinomas in the nonicteric stage by using MRCP followed by EUS. *Gastrointest Endosc.* 2009;70:29–36.
17. Okaya T, Hayashi S, Yamamoto K, Yamamori H, Abe M, Sugano I. Two cases of extrahepatic cholangiocarcinoma without jaundice. *J Jpn Surg Assoc.* 2009;70:2781–5.
18. Hiromatsu T, Hasegawa H, Sakamoto E, Komatsu S, Tabata T, Natsume S, Aoba T. A case of early bile duct carcinoma without jaundice diagnosed by endoscopic biopsy: a study of 73 resected cases in Japan. *J Jpn Biliary Assoc.* 2007;21:75–81.
19. Inui K. Biliary tract cancer: present status in early diagnosis and treatment. *Jpn J Gastroenterol.* 2006;103:495–500.

Wnt3a stimulates maturation of impaired neutrophils developed from severe congenital neutropenia patient-derived pluripotent stem cells

Takafumi Hiramoto^{a,b}, Yasuhiro Ebihara^{b,c,1}, Yoko Mizoguchi^d, Kazuhiro Nakamura^d, Kiyoshi Yamaguchi^e, Kazuko Ueno^f, Naoki Nariai^f, Shinji Mochizuki^{b,c}, Shohei Yamamoto^{b,c}, Masao Nagasaki^f, Yoichi Furukawa^e, Kenzaburo Tani^a, Hiromitsu Nakauchi^g, Masao Kobayashi^d, and Kohichiro Tsuji^{b,c}

^aDivision of Molecular and Clinical Genomics, Medical Institute of Bioregulation, Kyushu University, Higashi-ku, Fukuoka 812-8582, Japan; ^bDepartment of Pediatric Hematology/Oncology, Research Hospital, Divisions of ^cStem Cell Processing and ^dStem Cell Therapy, Center for Stem Cell Biology and Regenerative Medicine, and ^eDivision of Clinical Genome Research, Advanced Clinical Research Center, Institute of Medical Science, University of Tokyo, Minato-ku, Tokyo 108-8639, Japan; ^fPediatrics, Hiroshima University Graduate School of Biomedical and Health Sciences, Minami-ku, Hiroshima 734-8551, Japan; and ^gDepartment of Integrative Genomics, Tohoku Medical Megabank Organization, Tohoku University, Aramaki, Aoba-ku, Sendai 980-8573, Japan

Edited by George Q. Daley, Children's Hospital Boston, Boston, MA, and accepted by the Editorial Board January 4, 2013 (received for review October 1, 2012)

The derivation of induced pluripotent stem (iPS) cells from individuals of genetic disorders offers new opportunities for basic research into these diseases and the development of therapeutic compounds. Severe congenital neutropenia (SCN) is a serious disorder characterized by severe neutropenia at birth. SCN is associated with heterozygous mutations in the neutrophil elastase [elastase, neutrophil-expressed (ELANE)] gene, but the mechanisms that disrupt neutrophil development have not yet been clarified because of the current lack of an appropriate disease model. Here, we generated iPS cells from an individual with SCN (SCN-iPS cells). Granulopoiesis from SCN-iPS cells revealed neutrophil maturation arrest and little sensitivity to granulocyte-colony stimulating factor, reflecting a disease status of SCN. Molecular analysis of the granulopoiesis from the SCN-iPS cells vs. control iPS cells showed reduced expression of genes related to the wingless-type mmtv integration site family, member 3a (Wnt3a)/ β -catenin pathway [e.g., lymphoid enhancer-binding factor 1], whereas Wnt3a administration induced elevation lymphoid enhancer-binding factor 1-expression and the maturation of SCN-iPS cell-derived neutrophils. These results indicate that SCN-iPS cells provide a useful disease model for SCN, and the activation of the Wnt3a/ β -catenin pathway may offer a novel therapy for SCN with ELANE mutation.

apoptosis | unfolded protein response | SCN disease model

Severe congenital neutropenia (SCN) is a heterogeneous bone marrow (BM) failure syndrome characterized by severe neutropenia at birth, leading to recurrent infections by bacteria or fungi (1). SCN patients reveal an arrest in neutrophil differentiation in the BM at the promyelocyte or myelocyte stage (1), as well as a propensity to develop myelodysplastic syndrome and acute myeloid leukemia (2). Current treatment by high-dose granulocyte-colony stimulating factor (G-CSF) administration induces an increase in the number of mature neutrophils in the peripheral blood of most SCN patients (3). Although this treatment is curative for the severe infections, there is a concern that high-dose G-CSF may increase the risk of hematologic malignancy in these individuals (4).

Several genetic mutations have been identified in SCN patients. Approximately 50% of autosomal-dominant SCN cases were shown to have various heterozygous mutations in the gene encoding neutrophil elastase [elastase, neutrophil-expressed (ELANE)] (5, 6), a monomeric, 218-amino acid (25 kDa) chymotryptic serine protease (7) that is synthesized during the early stages of primary granule production in promyelocytes (8, 9). However, the mechanism(s) causing impaired neutrophil maturation in SCN patients remains unclear due to the current lack of an appropriate disease model.

Results and Discussion

In the present study, we generated induced pluripotent stem (iPS) cells from the BM cells obtained from an SCN patient with a heterologous ELANE gene mutation (exon 5, 707 region, C194X) (SCN-iPS cells) to provide the basis for an SCN disease model. The patient who donated BM cells recurrently suffered from severe infections without exogenous G-CSF administration, but the G-CSF administration once a week prevented his repeated infection. The SCN-iPS cells continued to show embryonic stem cell morphology after >20 passages and also expressed pluripotent markers (Fig. S1A). The silencing of exogenous genes and the capability to differentiate into three germ layers by teratoma formation were confirmed for each of the three SCN-iPS cell clones (Fig. S1B and C). Furthermore, the same ELANE gene mutation that was present in the patient persisted in the SCN-iPS cells (Fig. S1D). The SCN-iPS cells, as well as control iPS cells that were generated from healthy donors, had the normal karyotype (Fig. S1E) (10, 11) and no mutations in the mutation-sensitive region of the G-CSF receptor gene (12).

We first compared the hematopoietic differentiation from SCN-iPS cells with that from control iPS cells that were generated from healthy donors. SCN-iPS and control iPS cells were cocultured with a 15-Gy-irradiated murine stromal cell line (the AGM-S3 cell line), as reported (13). After 12 d, the cocultured cells were harvested, and the CD34⁺ cells separated from these cells (SCN-iPS-CD34⁺ and control iPS-CD34⁺ cells, respectively) were cultured in a hematopoietic colony assay by using a cytokine mixture (*Materials and Methods*). The number and size of the erythroid (E) and mixed-lineage (Mix) colonies derived from SCN-iPS-CD34⁺ cells (1×10^4 cells) were nearly identical to those of the corresponding colonies derived from control iPS-CD34⁺ cells (E colonies: SCN-iPS cells, 11.0 ± 3.0 , and control iPS cells, 11.4 ± 3.9 ; Mix colonies: SCN-iPS cells, 25.1 ± 7.2 , and control iPS cells, 17.4 ± 4.0) (Fig. 1B and C and Fig. S2A and B). However, the number of myeloid colonies derived from SCN-iPS-CD34⁺ vs. control iPS-CD34⁺ cells was significantly lower (SCN-iPS cells, 47.4 ± 19.5 ; control iPS cells, 127.8 ± 17.9 ; $P < 0.01$), and the size of the colonies was also smaller (Fig. 1A

Author contributions: T.H., Y.E., K.Y., S.M., S.Y., Y.F., K. Tani, H.N., M.K., and K. Tsuji designed research; T.H., Y.M., K.N., and K.Y. performed research; T.H., Y.E., Y.M., K.N., K.Y., K.U., N.N., S.M., S.Y., M.N., and K. Tsuji analyzed data; and T.H., Y.E., and K. Tsuji wrote the paper.

The authors declare no conflict of interest.

This article is a PNAS Direct Submission. G.Q.D. is a guest editor invited by the Editorial Board.

¹To whom correspondence should be addressed. E-mail: ebihara@ims.u-tokyo.ac.jp.

This article contains supporting information online at www.pnas.org/lookup/suppl/doi:10.1073/pnas.1217039110/-DCSupplemental.